AD-A100 888    HUGHES AIRCRAFT CO    TORRANCE CA ELECTRON DYNAMICS DIV        F/G 9/1
                LINEAR 1 KW MULTITONE TROPOSCATTER TWT.(U)
                MAY 81    A L ROUSSEAU                              DAAB07-77-C-2713
UNCLASSIFIED    EDD-W-07564-F                        DELET-TR-77-2713-F            NL

1 DF 1
AD A
·100888
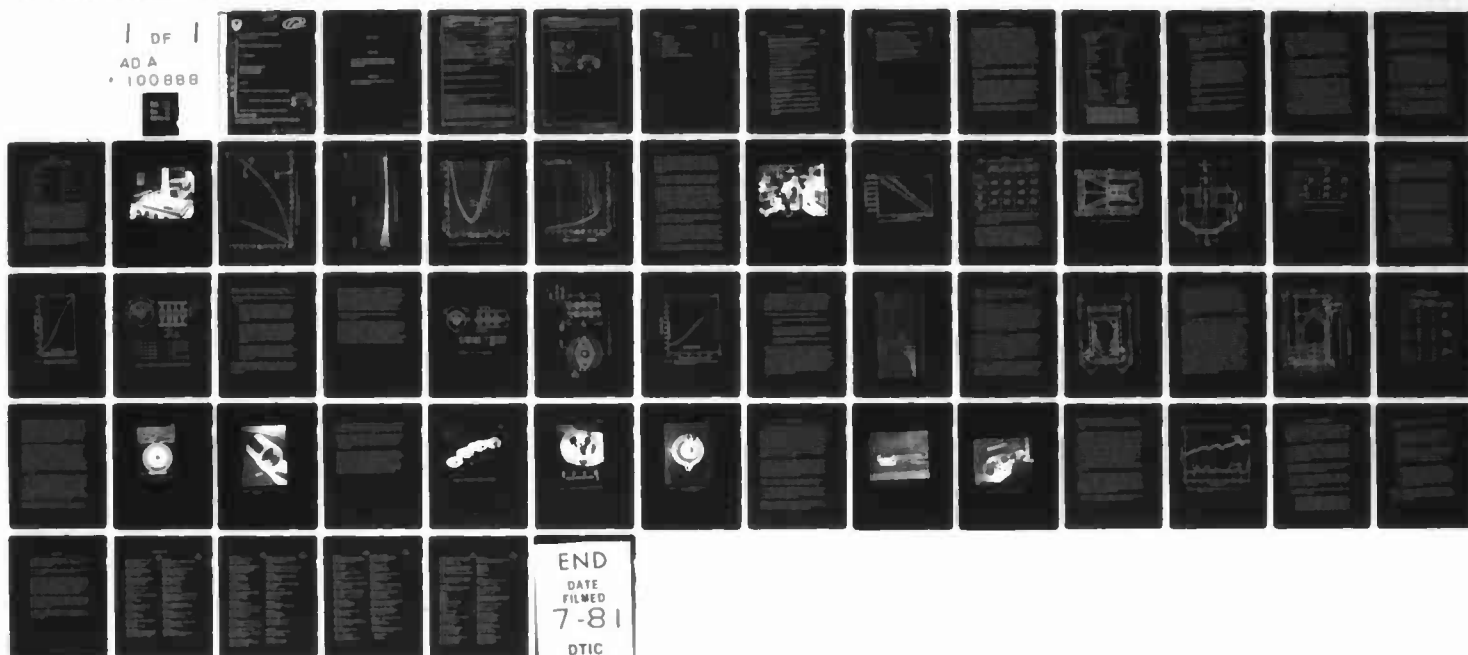
END
DATE
FILMED
7-81
DTIC

A

O 8

LEVEL *III*

AD A063 329

Research and Development Technical Report

DELET-TR-77-2713-F

# LINEAR 1 kW MULTITONE TROPOSCATTER TWT

A. L. ROUSSEAU

HUGHES AIRCRAFT COMPANY
Electron Dynamics Division
3100 West Lomita Boulevard
Torrance, California 90509

May 1981

Final Report for Period 1 September 1977 – 31 December 1980

DTIC
ELECTE
JUL 1 1981

D

Prepared For: Electronics Technology and Devices Laboratory

# ERADCOM
US ARMY ELECTRONICS RESEARCH AND DEVELOPMENT COMMAND
FORT MONMOUTH, NEW JERSEY 07703

81 7 01 050

# NOTICES

## Disclaimers

The citation of trade names and names of manufacturers in
this report is not to be construed as official Government
indorsement or approval of commercial products or services
referenced herein.

## Disposition

Destroy this report when it is no longer needed. Do not
return it to the originator.

| REPORT DOCUMENTATION PAGE | | READ INSTRUCTIONS BEFORE COMPLETING FORM |
|---|---|---|
| 1. REPORT NUMBER<br>DELET-TR-77-2713-F | 2. GOVT ACCESSION NO.<br>AD-A100888 | 3. RECIPIENT'S CATALOG NUMBER |
| 4. TITLE (and Subtitle)<br>LINEAR 1 kW MULTITONE TROPOSCATTER TWT | | 5. TYPE OF REPORT & PERIOD COVERED<br>Final Report<br>1 Sep 1977 to 30 Jan 1981 |
| | | 6. PERFORMING ORG. REPORT NUMBER<br>W-07564-F |
| 7. AUTHOR(s)<br>A. L. Rousseau | | 8. CONTRACT OR GRANT NUMBER(s)<br>DAAB07-77-C-2713 |
| 9. PERFORMING ORGANIZATION NAME AND ADDRESS<br>Hughes Aircraft Company<br>Electron Dynamics Division<br>3100 W. Lomita Blvd., Torrance, CA 90509 | | 10. PROGRAM ELEMENT, PROJECT, TASK AREA & WORK UNIT NUMBERS<br>1L7 62705 AH 94 B1-12 |
| 11. CONTROLLING OFFICE NAME AND ADDRESS<br>US Army Electronics Research & Development Command<br>ET&D Laboratory, ATTN; DELET-EM<br>Fort Monmouth, New Jersey 07703 | | 12. REPORT DATE<br>May 1981 |
| | | 13. NUMBER OF PAGES<br>45 |
| 14. MONITORING AGENCY NAME & ADDRESS(if different from Controlling Office) | | 15. SECURITY CLASS. (of this report)<br>UNCLASSIFIED |
| | | 15a. DECLASSIFICATION/DOWNGRADING SCHEDULE |

16. DISTRIBUTION STATEMENT (of this Report)

Approved for Public Release.
Distribution Unlimited.

17. DISTRIBUTION STATEMENT (of the abstract entered in Block 20, if different from Report)

18. SUPPLEMENTARY NOTES

19. KEY WORDS (Continue on reverse side if necessary and identify by block number)

High Power TWT
Intermodulation Distortion
Depressed Collector
High Efficiency Tube

20. ABSTRACT (Continue on reverse side if necessary and identify by block number)

This is the final report on a program to design, construct, and test a high power, G-Band TWT capable of amplifying multiple signals while minimizing any mixing products which results from non-linear operation. The approach is to operate the tube backed off from saturation to fulfill the distortion specification and incorporate a four-stage depressed collector to enhance the efficiency. → (over)

DD FORM<br>1 JAN 73 1473 EDITION OF 1 NOV 65 IS OBSOLETE

402638

cont

20. One experimental model of the 673H was produced.  Details of the designs of the electron gun, coupled-cavity interaction circuit, and multi-stage, air-cooled collector are presented.

Preliminary electrical performance data were obtained.

| Accession For | |
|---|---|
| NTIS GRA&I | ☒ |
| DTIC TAB | ☐ |
| Unannounced | ☐ |
| Justification | |

| By | |
|---|---|
| Distribution/ | |
| Availability Codes | |

| Dist | Avail and/or Special |
|---|---|
| A | |

DTIC
ELECTE
JUL 1 1981
D

D

## TABLE OF CONTENTS

# LIST OF ILLUSTRATIONS

iii

# LIST OF ILLUSTRATIONS (CONTINUED)

# 1.0  INTRODUCTION

The basic objective of this program was to demonstrate an optimum
traveling-wave tube (TWT) design for applications in tactical tropo-
scatter communications systems.  The design of this tube is based on
data presented in the Research and Development Technical Report ECOM-
75-1283-F.[1]  The primary design concept is to operate the tube below
saturation in order to achieve the low intermodulation (IM) require-
ments.  To achieve the required performance characteristics, the tube
is designed to operate approximately 6 to 7 dB below saturation.  At the
rated power of 1.0 kW minimum, the basic efficiency of the tube will be
approximately 4 percent.  To improve the overall efficiency of the tube,
a four-stage depressed collector is used to recover most of the kinetic
energy in the spent beam.  The original design study indicated that
use of this technique can increase the overall efficiency to a minimum
of 25 percent.

The specification for the multitone troposcatter TWT is presented in
Table 1.  Hughes has designated the model number 673H for the experi-
mental tube.

Periodic permanent magnet (PPM) focusing of the electron beam and air
cooling are objectives of the tube design.  PPM focusing used in place
of conventional solenoid focusing with the attendant solenoid power
supply increases overall efficiency and air cooling makes the tube more
compatible with existing troposcatter transmitters.  The 673H is
designed for both PPM focusing and air cooling.  However, this does
place stringent requirements on the thermal designs of both the RF
interaction circuit and the depressed collector.

The theoretical electrical characteristics of the tube were described
in detail in the earlier report, ECOM-75-1283-F.  The purposes of the

# TABLE 1

## SPECIFICATION FOR MULTITONE TROPOSCATTER TWT 673H

| Electrical Requirements | |
|---|---|
| Frequency Range | 4.4 to 5.0 GHz (Min) |
| Power Output CW | 1 kW (Min) |
| Gain | 40 dB (Min) |
| Instantaneous Bandwidth (-1 dB) | 15 MHz (Min) |
| Beam Voltage | -26 kV (Max) |
| Beam Current | 1.5 A (Max) |
| Efficiency (Note 1) | 25% (Min) |
| Intermodulation (Note 2) | -20 dBC |
| Output Load VSWR | 1.5:1 (Max) |
| Focusing | PPM (Objective) |
| Life | 10,000 Hrs. (Objective) |
| **Mechanical/Environmental** | |
| Size | To Be Determined |
| Weight | To Be Determined |
| Cooling | Air (Objective) |
| RF Input Connector | Type N Coax |
| RF Output Connector | WR-187 Waveguide/UG-149 Flange |
| Altitude (Operating) | 3100 Meters |
| Ambient Temperature (Operating) | $-50^{\circ}$C to $55^{\circ}$C |
| Mounting (Operating) | 0 to $15^{\circ}$ from Vertical |
| Shock (Non-operating) | 50 G, 1 msec |
| Vibration (Non-operating) | 5 to 55 Hz<br>1.02 cm Amplitude<br>5 ±0.5 Minutes |

Note:

1. The overall TWT efficiency is defined as:
   RF output power divided by the sum of beam input power, cooling power, focusing power, and heater power. The tube shall be capable of meeting the efficiency specified under conditions where the IM products are within the specified limits with 4 to 16 signals applied to the input.

2. The intermodulation products requirement will be met over any 15-MHz band in the 4.4 to 5 GHz frequency range. The 15-MHz band will be divided into 16 adjacent equal bandwidth channels. Anywhere from 4 to 16 of the channels will be occupied by carriers. The total intermodulation power in any occupied channel shall be 20 dB below the carrier in that channel. The carrier output power of all the occupied channels shall total 1 kW.

present program were to construct a tube having the previously determined design parameters and measure its operating performance. This effort consisted chiefly of the following areas:

1. An electron gun was scaled to the required beam size, area convergence and perveance, and mounted in an existing isolated anode support structure. It was evaluated in a demountable beam testing apparatus and used on the experimental 673H tube.

2. The RF interaction circuit and integral PPM focusing structure were designed.

3. The mechanical design of the four-stage depressed collector was accomplished, taking into account the voltage standoff and thermal dissipation requirements, using the electrode configuration that had been determined previously. Working out the assembly procedures and designing the brazing fixtures for this air cooled, multiple-stage collector were the most complicated and time consuming portions of the program. A collector was successfully constructed and placed on the 673H tube.

4. The overall packaging and cooling structure of the tube were designed.

5. The experimental tube was fabricated. Preliminary performance data were obtained.

Various aspects of the details of the 673H tube design, construction and testing will be described in the following sections.

3

## 2.0 ELECTRON GUN

In determining the design for the multitone tube, parameters were chosen
to achieve the highest overall efficiency within the distortion speci-
fication of 20-dB carrier-to-IM (C/IM) power ratio. C/IM ratio requires
operating the tube 6 to 7 dB below saturation to meet the C/IM require-
ment and using a four-stage depressed collector to increase the overall
efficiency. For high overall efficiency it is necessary to have a
relatively high (3 to 5%) basic tube efficiency at the backed-off con-
dition, good beam transmission to the collector, and effective collector
performance.

To ensure good beam transmission in a PPM focused device, the focusing
quality parameter $\lambda_p/L$ (plasma wavelength divided by the magnetic period)
is made 3.5 or larger. With a given operating voltage and current, the
interaction strength is then maximized by choosing a beam hole as
small as possible consistent with the $\lambda_p/L$ constraint, assuming a beam
radius to drift tube hole radius (b/a) of 0.6.

A calculation of Pierce's gain parameter C was performed as a function
of the beam voltage, assuming a constant beam power of 20 kW and using
a minimum beam hole size consistent with $\lambda_p/L = 3.8$. Under these con-
ditions the C parameter was nearly independent of voltage. The choice
of operating voltage was, therefore, made with good collector perform-
ance in mind. A high-voltage, low-perveance design has smaller space
charge density in the beam, which tends to make it easier to sort the
electrons in the collector according to their energy. Furthermore, a
high voltage permits a small beam hole with a low radial propagation
parameter γa. The low space charge density helps to reduce the RF
defocusing in the beam, resulting in improved beam transmission and
decreased spread in electron trajectory angles. Both of these condi-
tions are desirable for high efficiency enhancement with the multistage

collector.  A high voltage also increases the axial dimensions of the
interaction circuit, which improves its thermal dissipation capability.

The final operating parameters chosen for the 673H are a beam voltage
of 25 kV and a current of 1.3 A.  The electron gun is a Pierce[2] type
convergent flow gun with an area compression of 16:1 to assure low
cathode emission current density and long life.  The required charac-
teristics of the gun, designated the Hughes 238B, are summarized in
Table 2.

For the gun design, empirical design curves were used that depict
the relationships between perveance, cathode half-angle, and beam size
for the desired cathode diameter.  The electrolytic tank, shown in
Figure 1, was then used to establish the electrode configuration and
relative spacings.  These determinations are made by first computing
what the theoretical beam edge potential distribution should be, given
the gun perveance, the cathode radius and $\bar{r}_c/\bar{r}_a$ (the ratio of the
spherical cathode radius to the effective spherical anode radius).
Then models of the focus electrode and anode are adjusted until the
best possible match to the theoretical beam edge distribution is
achieved.  The result of this procedure is shown in Figure 2.

Next, the Hermansfeldt[3] computer program, which solves Poisson's equa-
tion for a cylindrical boundary problem, was used to predict the axial
potentials, perveance, and nonthermal electron trajectories.  A com-
puter generated description of the 238B gun is shown in Figure 3.

When the perveance parameter and computer perveance agreed, another
computer program,[4,5] which takes into account thermal electron velocity
effects, used the axial potentials, the relevant gun parameters, and
an assumed magnetic field distribution to compute the focused electron
beam shape.  The electrostatic beam envelopes were also predicted for a

5

## TABLE 2

### 238B ELECTRON GUN DESIGN PARAMETERS

| | |
|---|---|
| Cathode Voltage | -25 kV |
| Cathode Current | 1.3 A |
| Perveance | $0.33 \times 10^{-6}$ |
| Cathode Loading | $1.1 \text{ A/cm}^2$ |
| Nominal Beam Diameter | 0.121 Inch (3.07 mm) |
| Area Compression | 16:1 |
| Cathode Material | Impregnated Tungsten |
| Magnetic Field | PPM |
| Magnetic Period | 1.036 Inch (26.31 mm) |

thermal beam using this method. Figure 4 shows the computer generated plots for five electrostatic beam envelopes of the 238B electron gun. The envelope containing 99.5 percent and 95 percent of the beam current are labeled $r_{99.5}$ and $r_{95}$ respectively. The beam radii where the current density is 1/10 and 1/20 the peak current density are indicated by $r_{1/10}$ and $r_{1/20}$ respectively. The fifth radius, $r_o$, is the statistically averaged beam radius. Typically, the program computes the minimum beam position about 10 percent less than is measured; thus the cathode valley to the bean minimum position was predicated to be 1.59 inches.

An optimized computer run for the focused beam is shown in Figure 5. The focusing field for this case has a peak amplitude of 1350 gauss. This optimum focusing occurs when the first magnetic field is 0.240 inch downstream from the electrostatic beam minimum position.

6

E1035
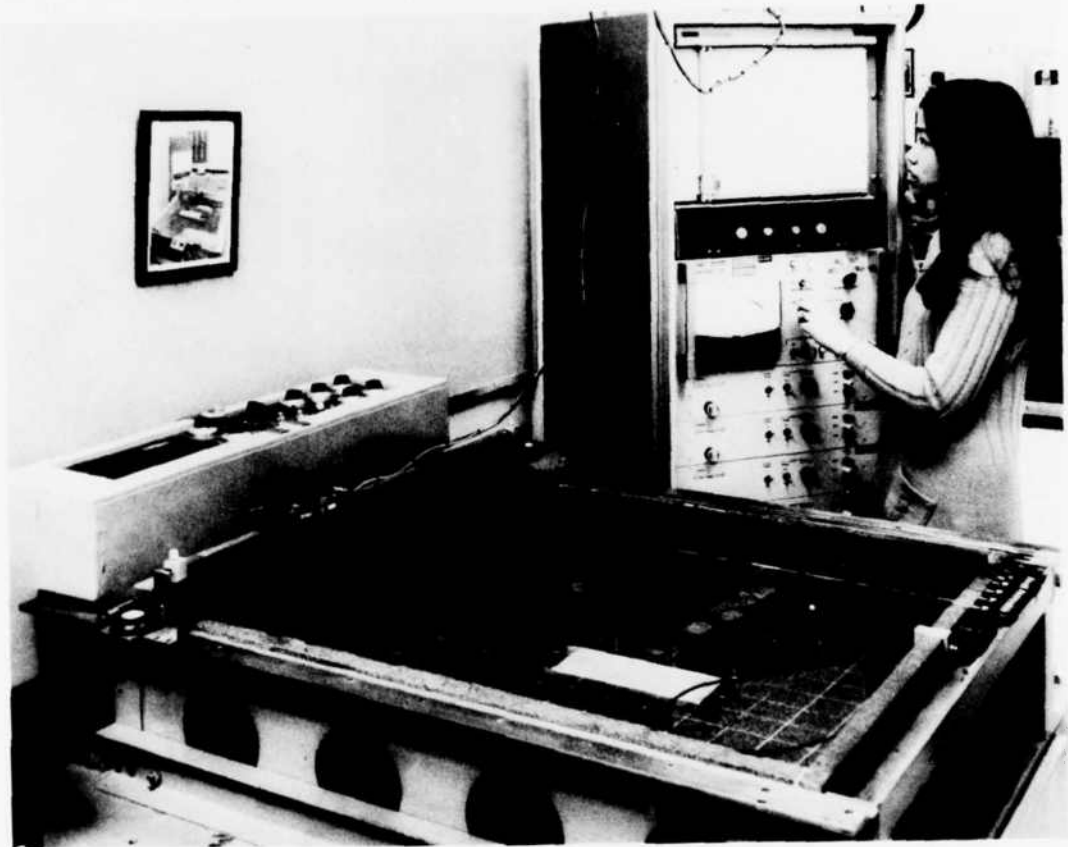
Figure 1    Electrolytic tank.
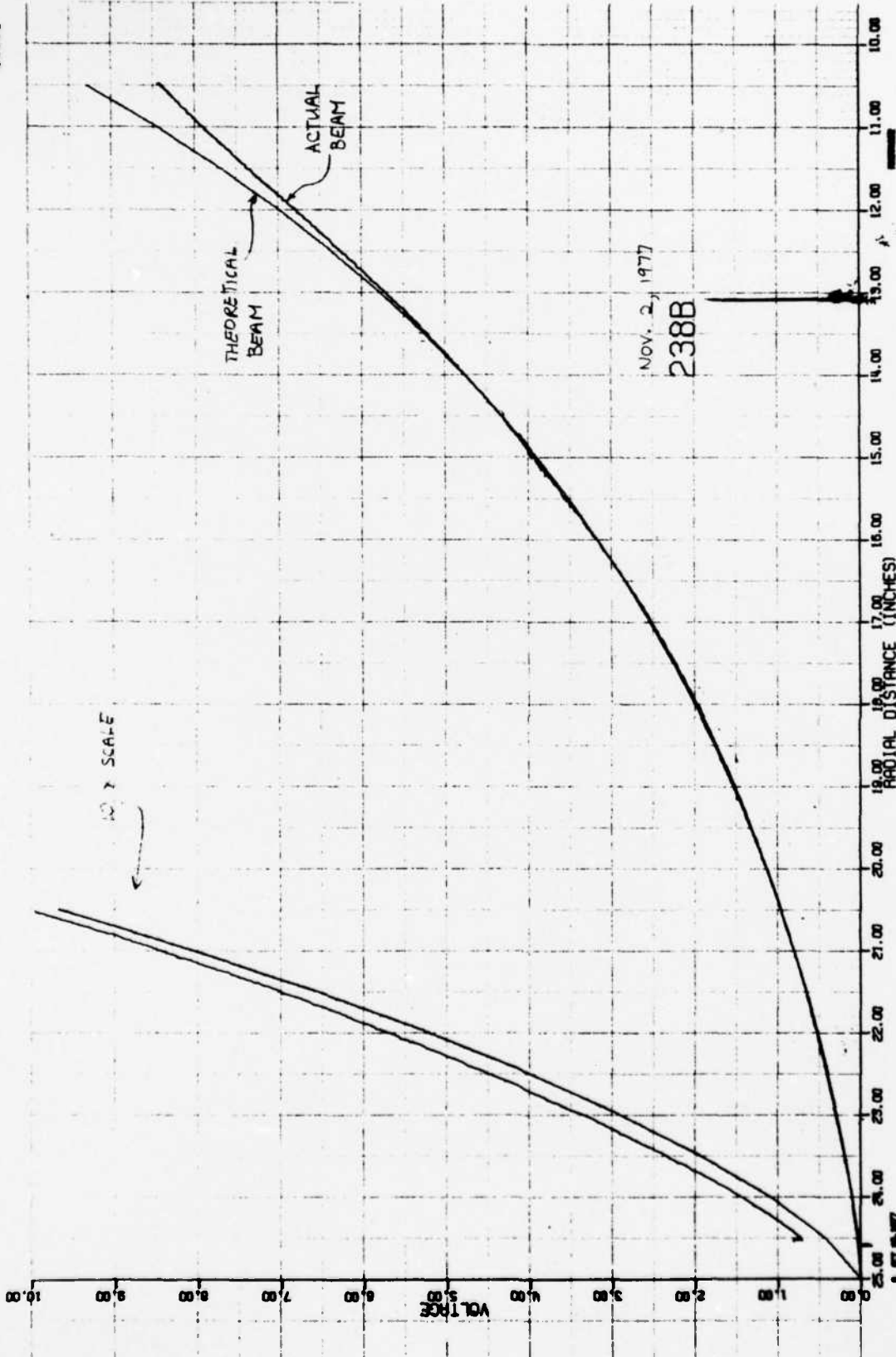
Figure 2   Theoretical and electrolytic tank measurements of beam edge potential for 238B electron gun.

8

G8996

MESH UNITS/DIVISION

MESH UNITS/DIVISION

238B GUN RUN2
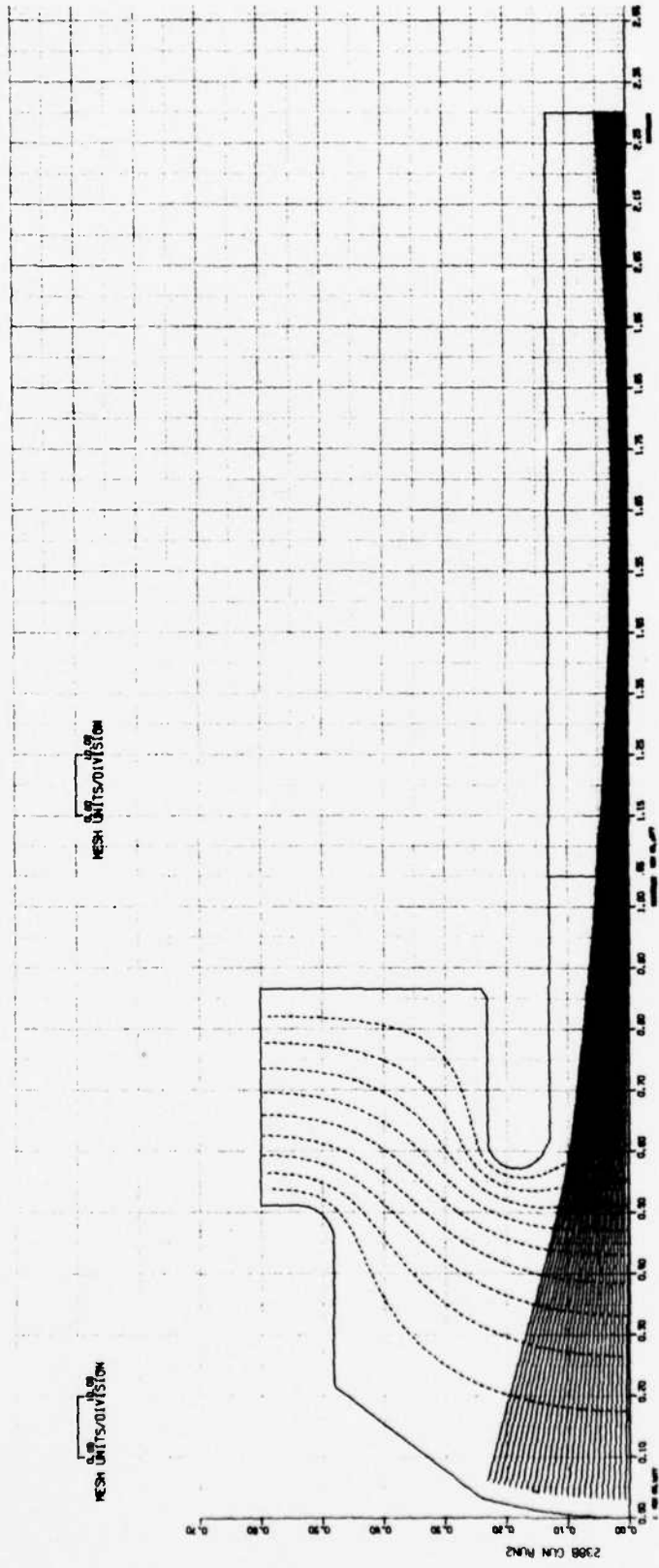
Figure 3    Computer generated electron trajectories and potential
distribution of 238B electron gun.

9
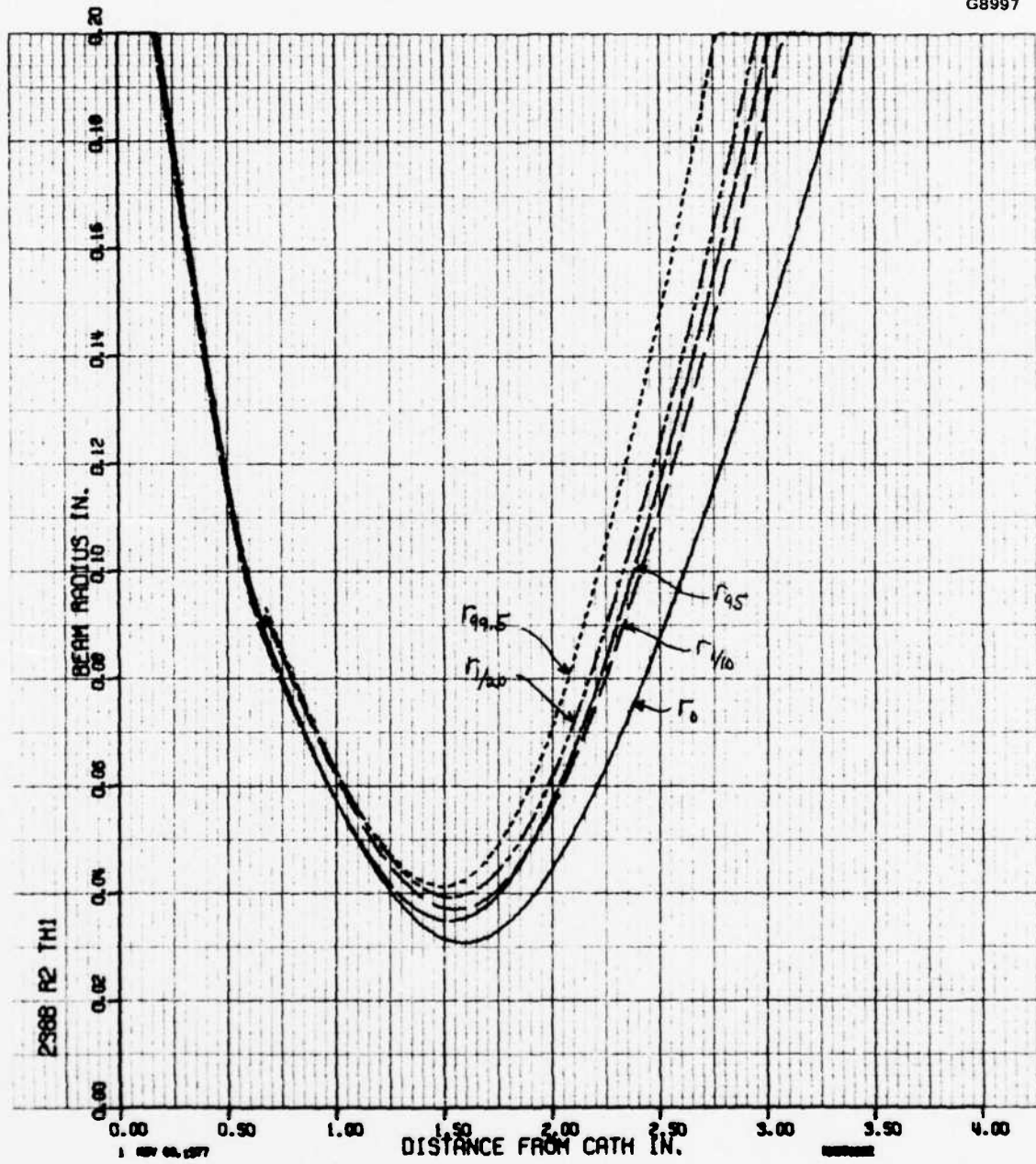
Figure 4    Computed electrostatic beam envelopes of 238B gun.

10
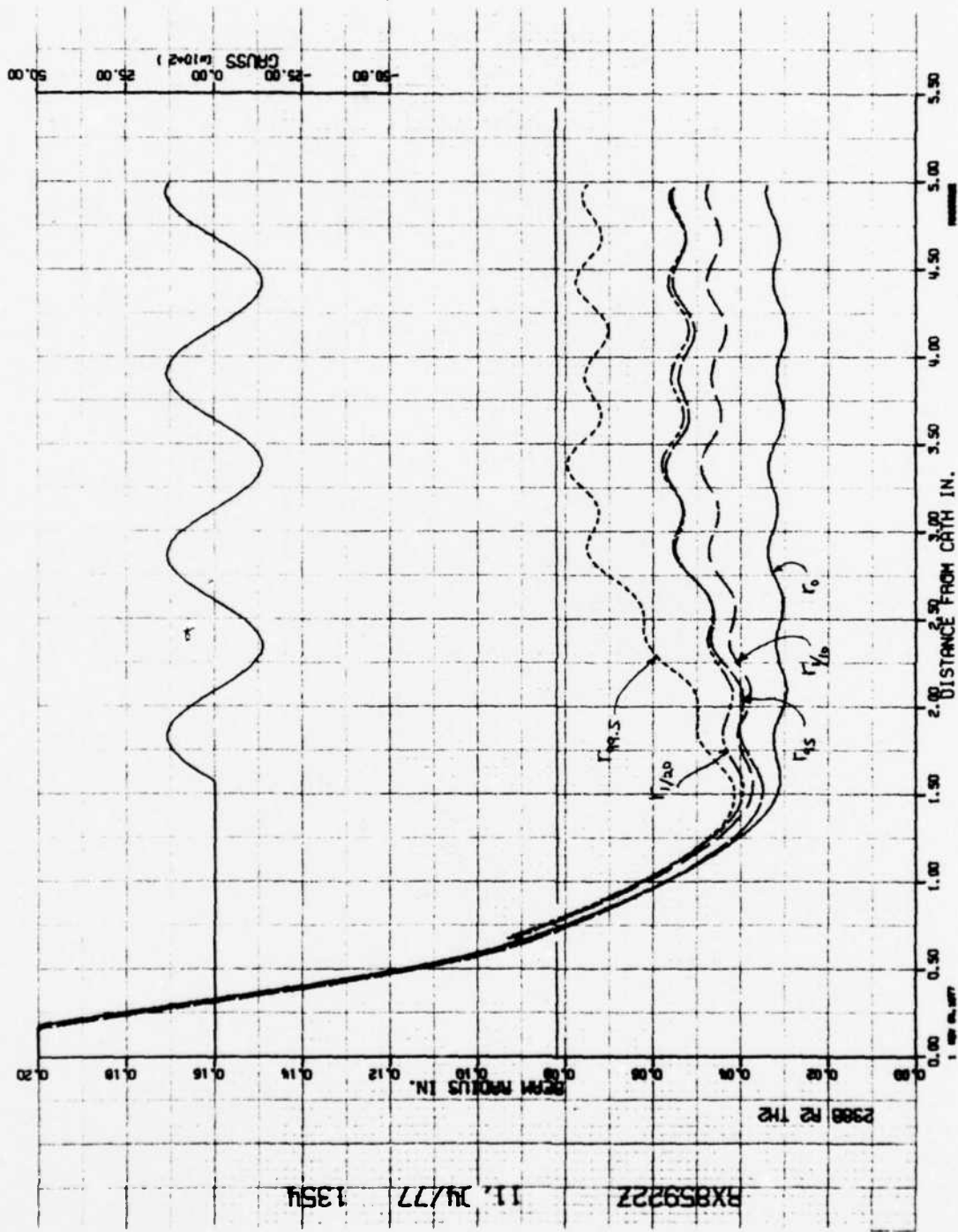
Figure 5    Focused beam characteristics for 238B electron gun.

11

In order to verify the design, parts were ordered to build an "A" scale gun for checking in the beam analyzer. For the 238A gun, the 238B gun just discussed was scaled by a factor of 0.911 in order to achieve a scaled cathode diameter of 0.440 inch (11.18 mm), which is compatible with the analyzer test fixtures. The test setup is shown in Figure 6.

Two versions of the 238A gun, differing only in cathode-to-anode spacing, were checked. The 238A gun number 1 had a measured perveance of 0.30 microperv rather than the design perveance of 0.33 microperv.

The cathode-to-anode spacing was then decreased by 0.010 inch. The measured perveance of this 238A gun number 2 was 0.33 microperv. The beam minimum occurs 1.432 inches (36.37 mm) from the cathode valley. The measured $r_{1/20}$ is 0.040 inch (1.02 mm) at 10 kV. ($r_{1/20}$ is the beam radius where the current density is 1/20 the peak current density.) 10 kV is the maximum test voltage that can be used with the demountable analyzer. The predicted $r_{1/20}$ at an operating voltage of 25 kV is 0.0355 inch (0.902 mm). A plot of beam voltage versus $r_{1/20}$ is shown in Figure 7.

The final 238B gun design was obtained by scaling the dimensions of the 238A gun number 2 by 1.0977. The relevant theoretical and experimental gun parameters are summarized in Table 3.

The detail mechanical design of the 238B gun was completed by adapting the 238B electrodes to a standard isolated anode insulator assembly with appropriate corrections to account for the differential expansions of the various support elements of the gun at operating temperature. The gun layout is shown in Figure 8. The dimensions of the electrodes are presented in Figure 9.

The first electron gun for the tube in the modulating anode configuration was evaluated in the demountable beam analyzer in order to compare

12
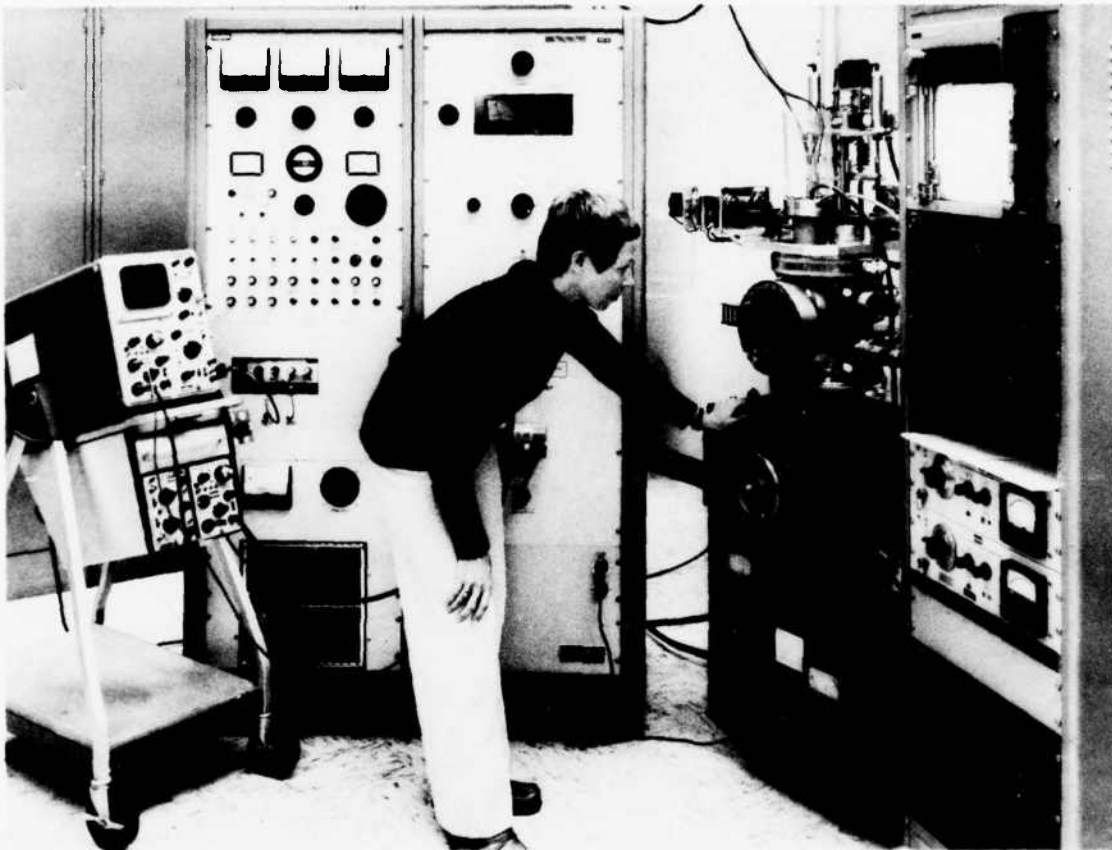
Figure 6    Electrostatic demountable beam analyzer No. 1.
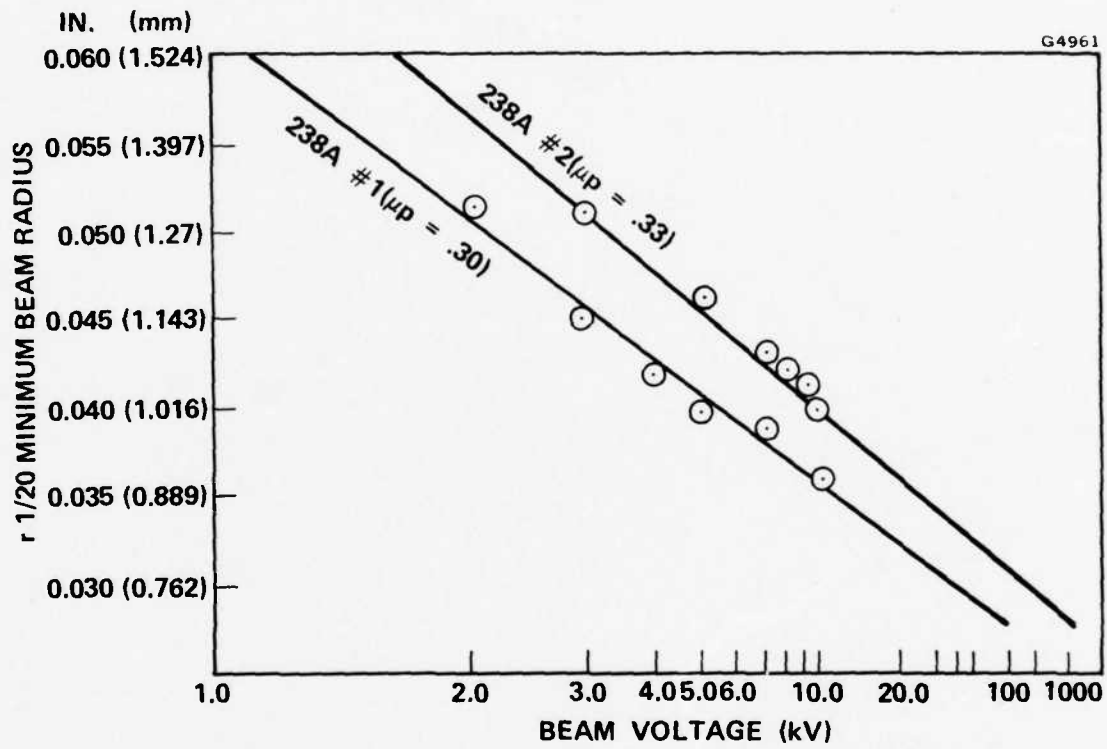
Figure 7    238A demountable guns $V_b$ vs r 1/20.

14

## TABLE 3

### SUMMARY OF THEORETICAL AND EXPERIMENTAL 238 GUN PARAMETERS

| | Original Computed 238B Design | 238A Scaled from Original 238B | 238A Number 2 Test Results | Final 238B Scaled from 238A No. 2 |
|---|---|---|---|---|
| Perveance (Micropervs) | 0.33 | 0.33 | 0.33 | 0.33 |
| $r_{1/20}$ Electro-static at 25 kV $\frac{\text{inch}}{(\text{mm})}$ | $\frac{0.0392}{(0.996)}$ | $\frac{0.0357}{(0.907)}$ | $\frac{0.0328}{(0.833)}$ | $\frac{0.0360}{(0.914)}$ |
| $r_{99.5}$ Focused at 25 kV $\frac{\text{inch}}{(\text{mm})}$ | $\frac{0.0796}{(2.022)}$ | $\frac{0.0725}{(1.842)}$ | $\frac{0.0666}{(1.692)}$ | $\frac{0.0731}{(1.857)}$ |
| Cathode valley to beam minimum $\frac{\text{inch}}{(\text{mm})}$ | $\frac{1.59}{(40.39)}$ | $\frac{1.45}{(36.83)}$ | $\frac{1.43}{(36.32)}$ | $\frac{1.57}{(39.88)}$ |

the actual gun to the scaled version and determine whether there were
any major differences introduced by installing the electrodes in the
actual tube mounting structure. The results were very close to the
earlier calculated values.

The gun was operated at a heater voltage of 12.5V which maintained a
cathode temperature of 1100°C brightness, as measured on the tungsten
body of the impregnated cathode pellet. The data were taken at cathode
voltages of 11 kV and lower, and then extrapolated to 25 kV so as not to
exceed the voltage standoff capability of the demountable test equipment.
The results are summarized in Table 4. The 238B design numbers are
the values scaled from the earlier 238A measurements. The 238B test

G5039
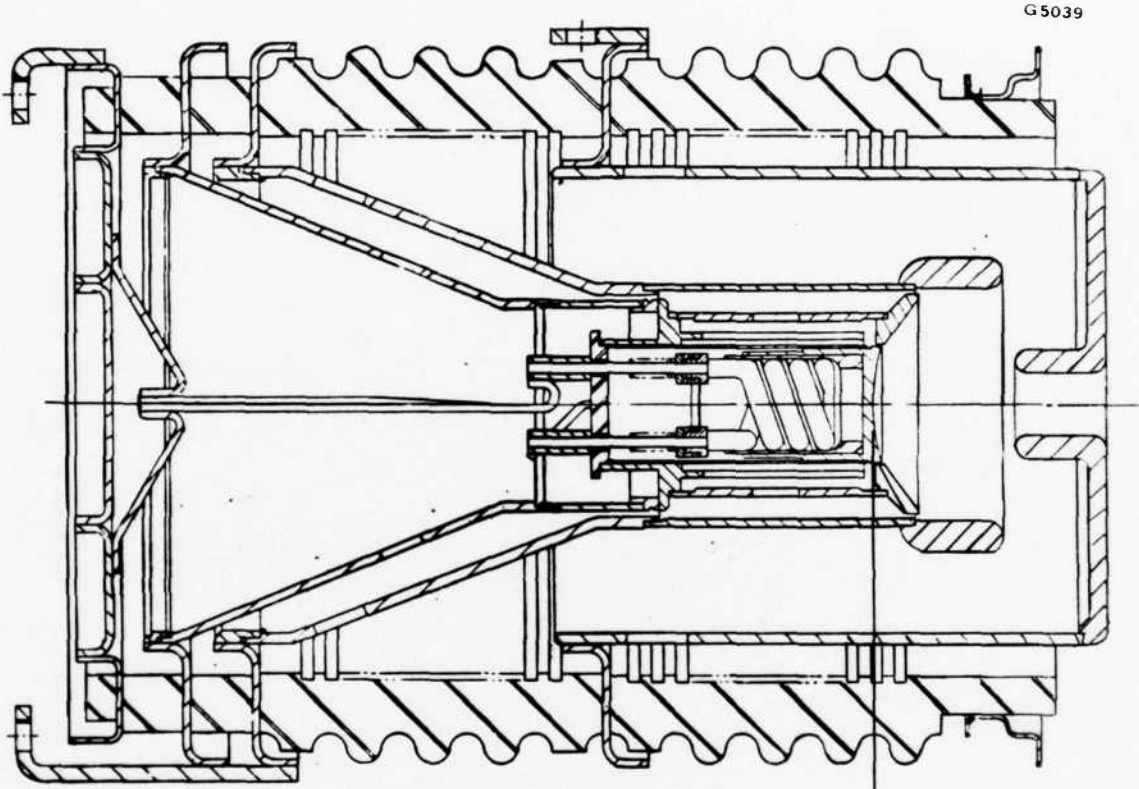
Figure 8    238B isolated anode electron gun.

16

G8993

0.964 (24.5mm)
DIA

0.261 DIA
(6.63mm)

0.940 (23.9mm)
SPH. R.

0.293
(7.44mm)

0.876
(22.3mm)

0.525
(13.3mm)

0.483 (12.27mm)
DIA
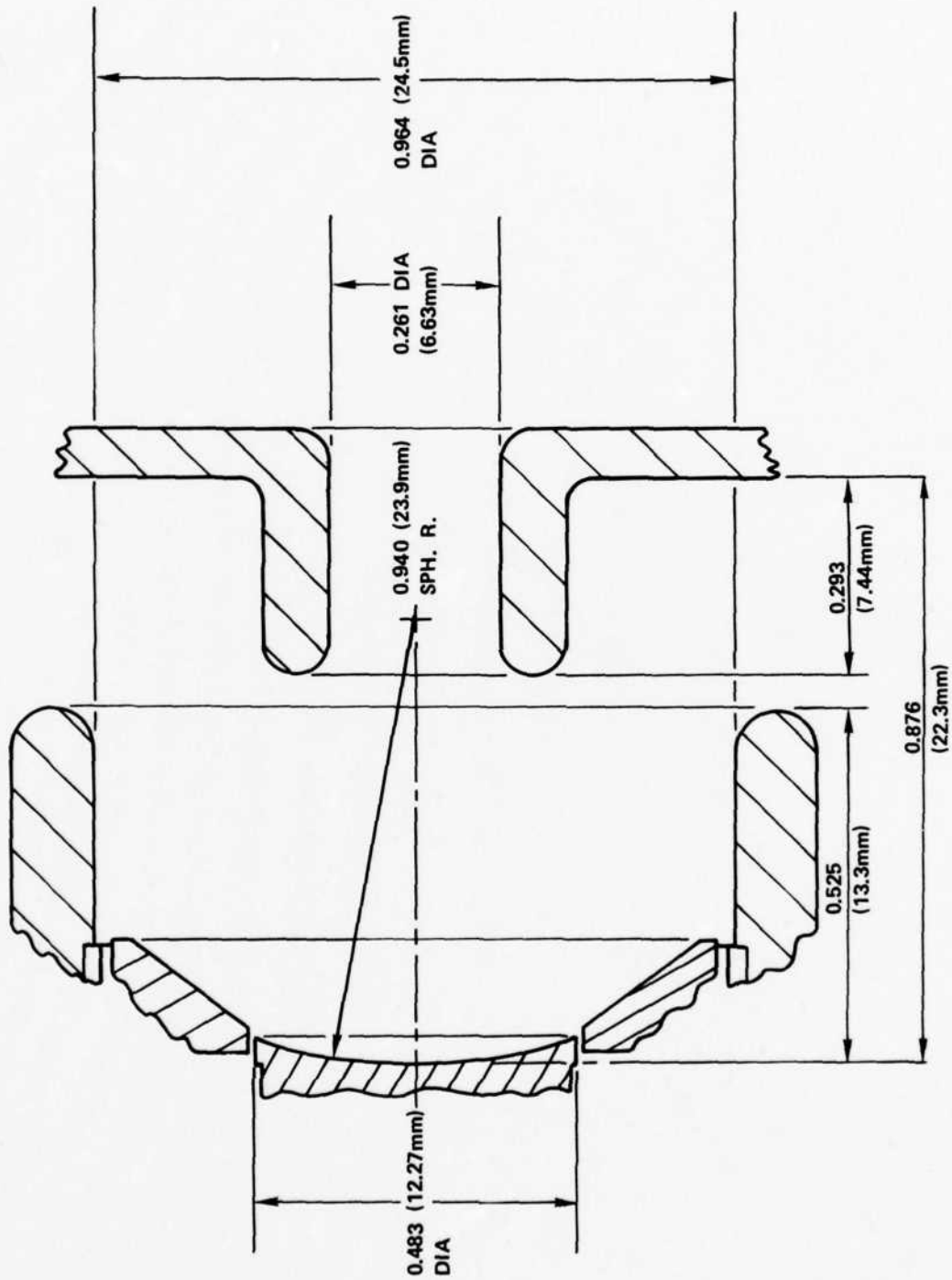
Figure 9  Electron gun dimensions.

17

TABLE 4

238B MODULATED ANODE ELECTRON GUN TEST RESULTS

| | 238B Design | 238B Test |
|---|---|---|
| Perveance (Micropervs) | 0.33 | 0.32 |
| $r_{/120}$ Electrostatic $\frac{\text{inch}}{\text{(mm)}}$ at 25 kV | $\frac{0.0360}{(0.914)}$ | $\frac{0.037}{(0.940)}$ |
| $r_{99.5}$ Focused $\frac{\text{inch}}{\text{(mm)}}$ at 25 kV | $\frac{0.0731}{(1.857)}$ | ═══ |
| Cathode Valley $\frac{\text{inch}}{\text{(mm)}}$ to Beam Minimum | $\frac{1.57}{(39.88)}$ | $\frac{1.596}{(40.54)}$ |

numbers are the values measured on the completed gun assembly extra-polated to 25 kV.

This electron gun was later installed on the completed 673H tube.

18

## 3.0  INTERACTION CIRCUIT

The general circuit parameters for the multitone tube were determined
in the previous study program.[1]  The theoretical phase-versus-frequency
($\omega$-$\beta$) characteristic used in the study is shown in Figure 10.  The basic
cavity configuration is presented in Figure 11.  Values of the outer
diameter, coupling hole angle, and cavity gap are approximate; these
dimensions must be adjusted during cold testing to give the desired
$\omega$-$\beta$ response.

In a PPM focused coupled-cavity TWT, the cavity walls are made of iron.
They serve as pole pieces for concentrating the magnetic field in the
proximity of the electron beam.  The focusing magnets are situated
between adjacent pole pieces and just outside the copper spacers, which
form the cavity outer diameter.  Cooling of the pole pieces is critical
because runaway conditions can be encountered if the temperature of the
pole piece is allowed to approach the Curie temperature of the iron.
The beam and circuit parameters were chosen with the aim of providing
excellent beam transmission.  Nevertheless, it must be assumed that
some beam power will be intercepted on the interaction circuit.

Calculations were made of the temperature rise from the outer cavity
diameter to the tip of the drift tube ferrule, where the beam is inter-
cepted.  This temperature rise will depend upon the amount of the
intercepted beam power.  For the calculation a worst case transmission
of 98 percent was assumed with a total beam power of 32.5 kW.  This
interception will be spread along the circuit.  It was also assumed
that, at most, one-tenth of the total intercepted power of 65 W hits
any one ferrule.  (A beam scraper section is planned at the input of
the circuit near the gun end, so possible higher interception in that
region is not considered here.)  For iron cavity walls, the temperature
rise was calculated to be 600°C.  The actual ferrule tip temperature
must be increased by the $\Delta T$ from the cavity outer diameter to the

19
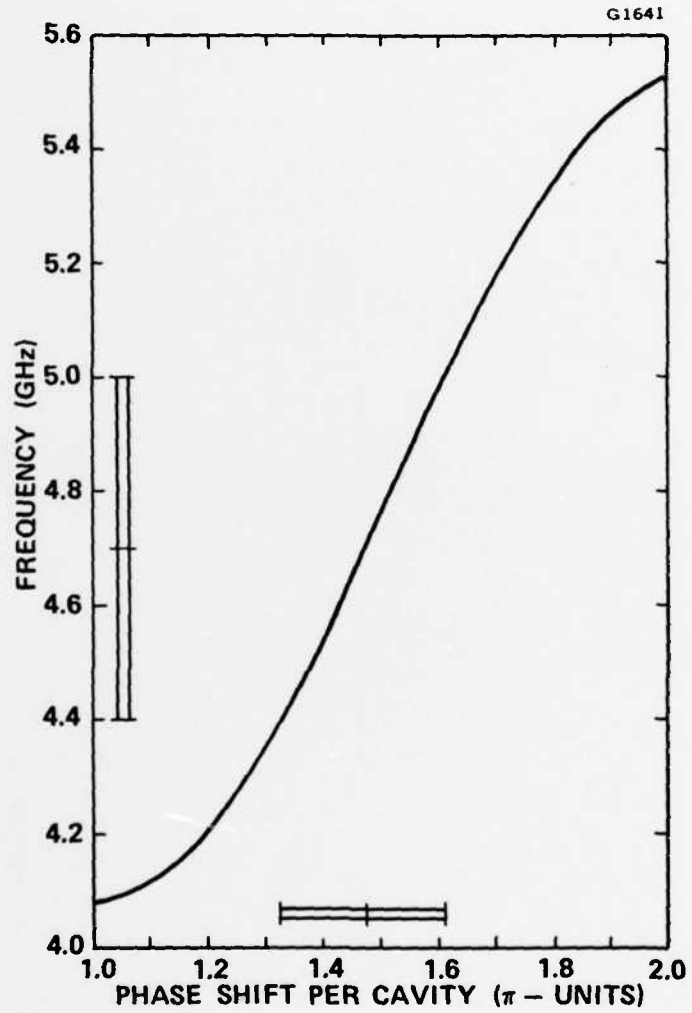
Figure 10    Theoretical frequency-vs-phase ($\omega\beta$)
characteristic of interaction circuit.
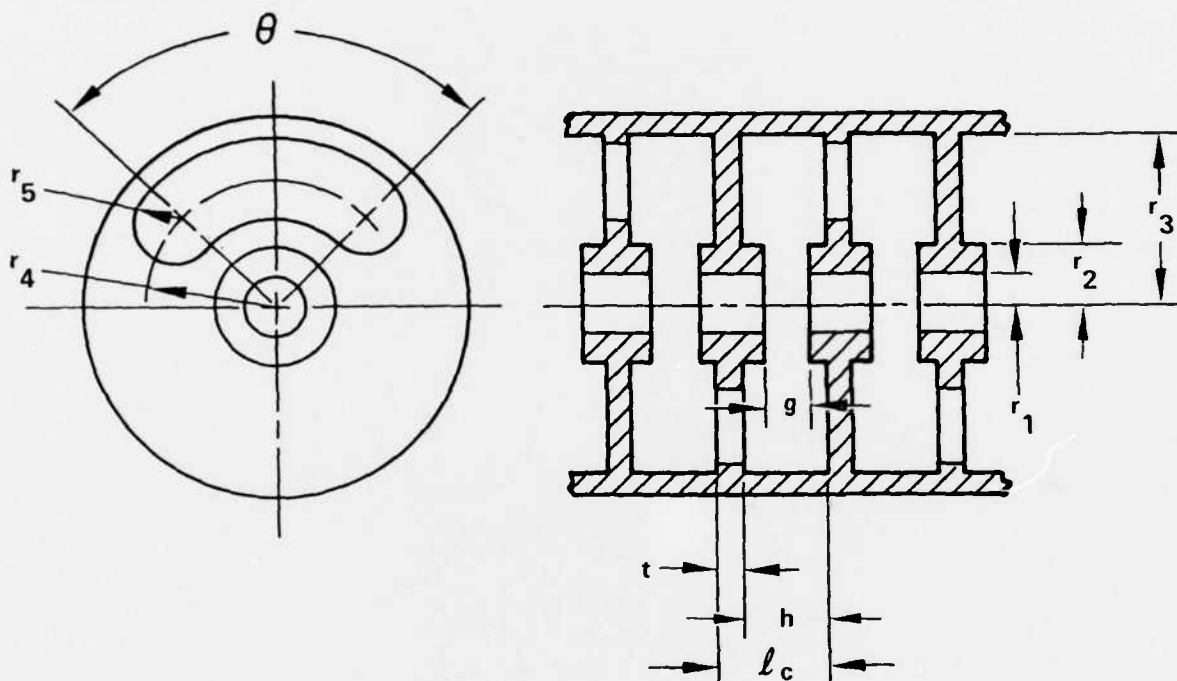
20

G1327

$$2r_1 = \ .202 \text{ in. (5.13 mm)} \qquad \ell_c = .518 \text{ in. (11.16 mm)}$$

$$2r_2 = \ .282 \text{ in. (7.16 mm)} \qquad t = .080 \text{ in. (2.03 mm)}$$

$$2r_3 = 1.182 \text{ in. (30.02 mm)} \qquad g = .135 \text{ in. (3.43 mm)}$$

$$2r_4 = \ .790 \text{ in. (20.07 mm)} \qquad \theta = 100^\circ$$

$$2r_5 = \ .390 \text{ in. (9.91 mm)} \qquad h = .438 \text{ in. (11.13 mm)}$$

Figure 11   Schematic of coupled-cavity slow-wave circuit.

21

coolant. This value of temperature rise would be completely unsatisfactory even if liquid cooling were substituted for air cooling.

To improve the thermal capability of the circuit, the following changes were made:

1.  The cavity walls were increased in thickness from 0.080 to 0.118 inch. The thicker cavity wall results in a slightly reduced circuit impedance, which lowers the calculated tube efficiency by about 0.4 percentage point to approximately 26.5 percent minimum overall efficiency with collection depression.

2.  The ferrule radial thickness was not increased because that would have reduced the impedance and efficiency more drastically. However, the ferrule outer diameter was tapered to a larger diameter at the base of the ferrule, where it joins the cavity wall. This larger diameter improves the thermal conduction without appreciably affecting the interaction impedance.

3.  Copper laminations were introduced on the iron pole pieces. The copper laminations are each .020 inch thick; the remaining iron is .078 thick. This technique is effective because copper has a thermal conductivity approximately seven times as high as iron.

The incorporation of these modifications in the circuit structure has reduced the calculated temperature rise from the cavity outer diameter to the ferrule tip to 66°C. This is a reasonable value for an air cooled tube.

Phase shift measurements were made on experimental cold test circuit structures to obtain the exact circuit dimensions. In these measurements, the drift tube ferrule gap and the size of the coupling hole are varied until the desired passband has been obtained. Resonant loss material was included in these cold test circuits to properly simulate the actual tube circuit. (The loss material lowers the passband by about 250 MHz.) The final dimensions are shown in Figure 12. A layout of the completed circuit assembly is presented in Figure 13.

The measured $\omega$-$\beta$ characteristic for the actual 673H circuit is presented in Figure 14.

Frequency perturbation measurements with a dielectric rod were made to determine the circuit interaction impedance. The small signal gain was then calculated, taking into account the measured circuit impedance and electron beam characteristics. These calculations indicated that the gain will be approximately 0.1 dB per cavity higher than had been assumed in the original study. The circuit configuration has, therefore, been chosen to have 16 cavities in the driver section and 17 cavities in the output section, not including termination and matching cavities.

G4962
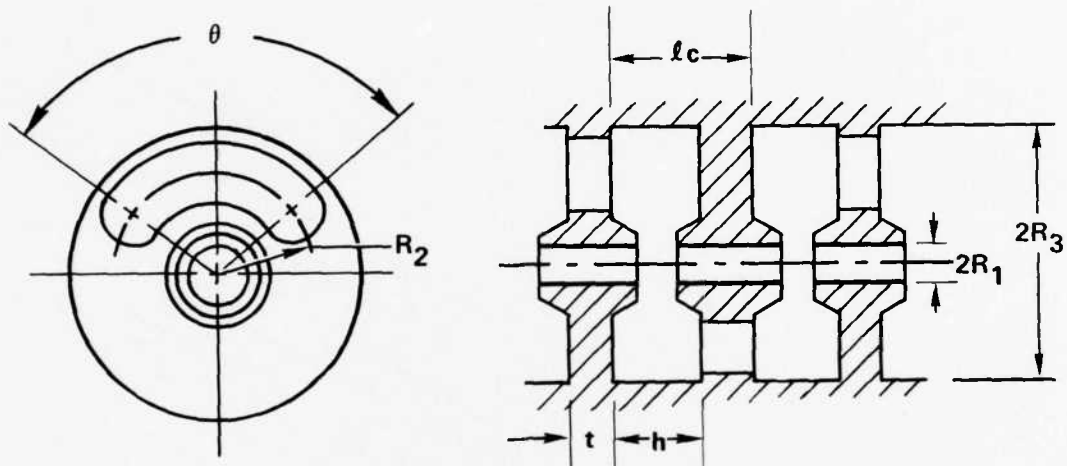
$2R_1 = 0.202$ in. (5.13 mm)     $\ell c = 0.518$ in. (13.16 mm)
R2  $= 0.385$ in. (9.78 mm)       h  $= 0.400$ in. (10.16 mm)
$2R_3 = 1.100$ in. (27.94 mm)     t  $= 0.118$ in. (3.00 mm)
                                  $\theta = 110^o$

Figure 12   673H cavity dimensions.
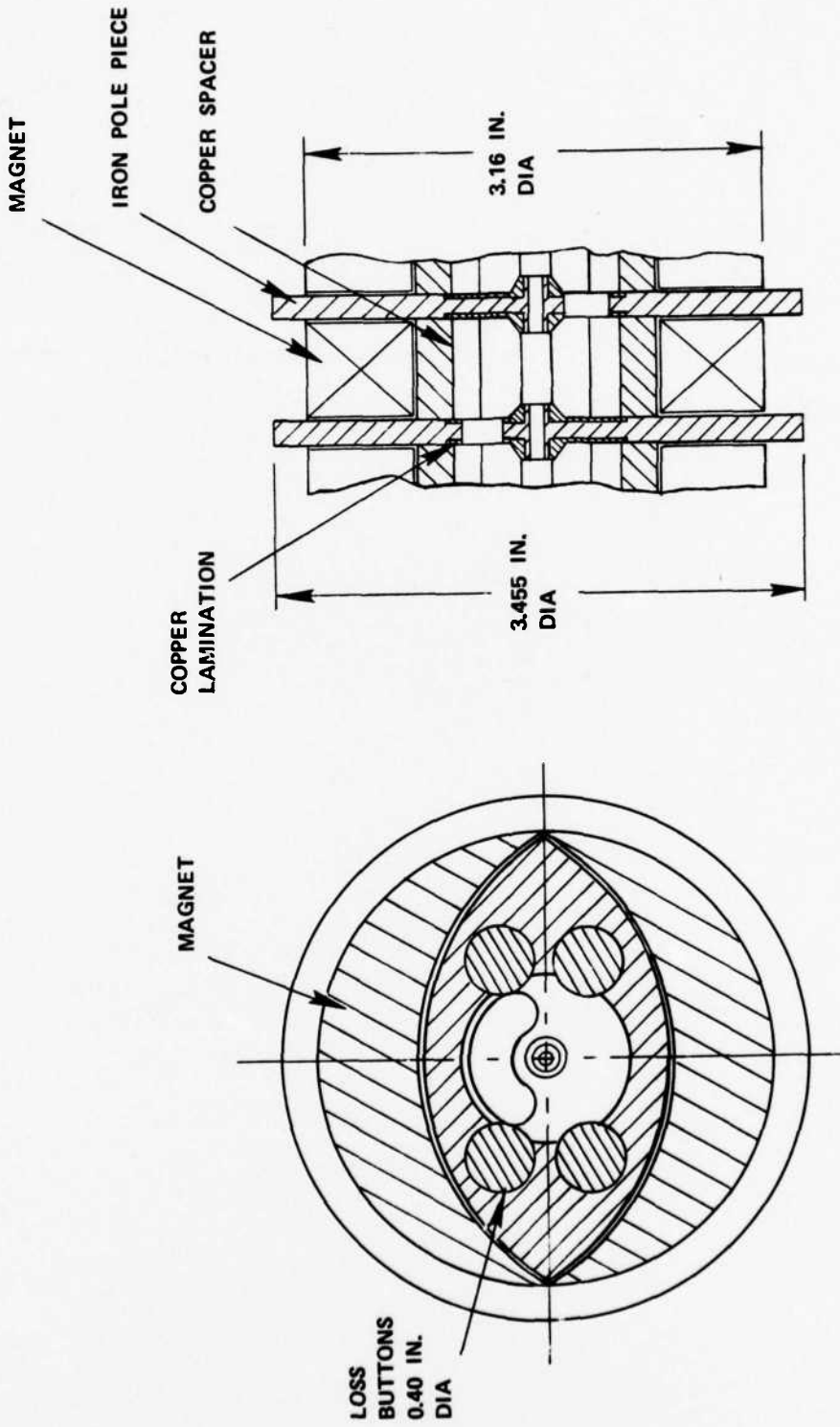
Figure 13   Schematic layout of 673H circuit section.

25
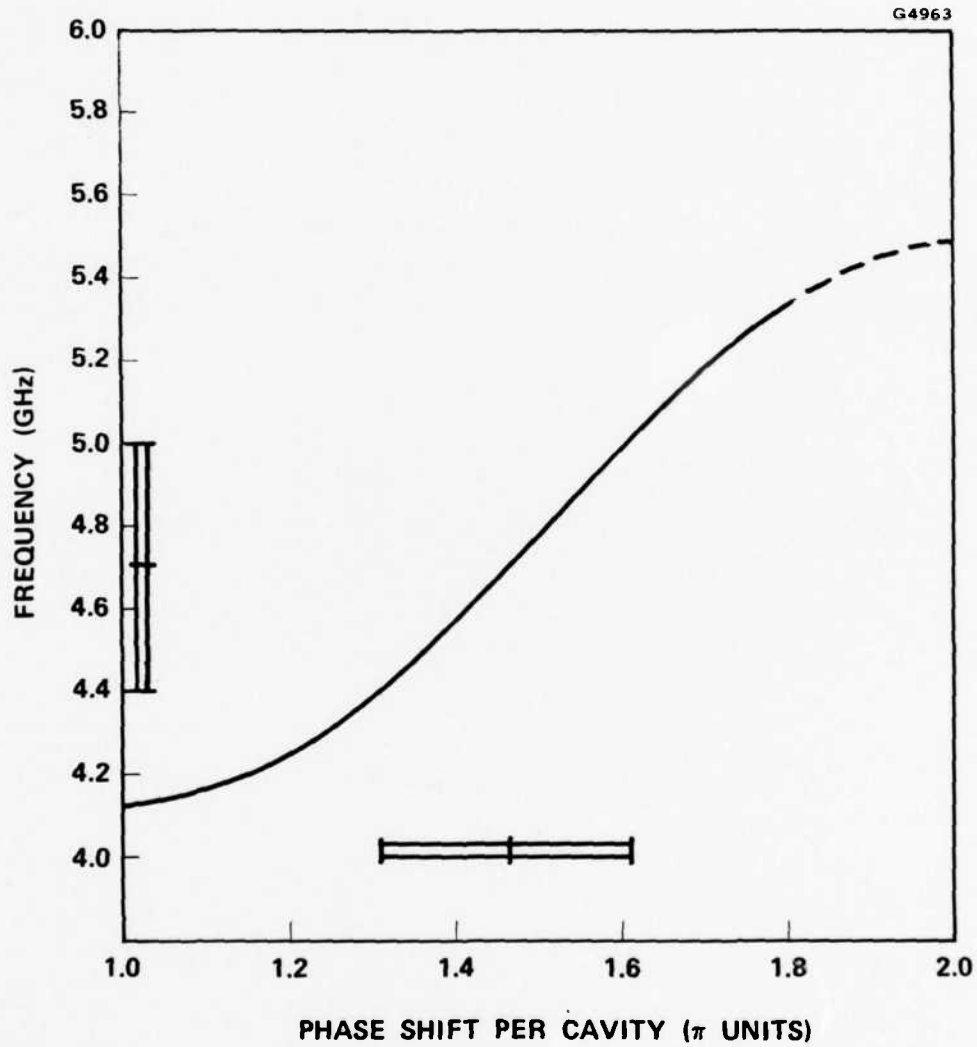
Figure 14  Measured frequency vs phase ($\omega\beta$) characteristic of interaction circuit.

## 4.0 COLLECTOR DESIGN

The multistage depressed collector is the key element in achieving high overall efficiency on the 673H. The basic efficiency of the tube has been theoretically predicted to be a minimum of 4 percent across the frequency range of 4.4 to 5.0 GHz. To increase the overall efficiency of the tube to 25 percent will require that the spent beam be collected in a manner which will recover most of its kinetic energy.

The multistage collector has three electrical functions:

1.  To sort the electrons in the spent beam according to their energies

2.  To slow the electrons so that they may be collected with their lowest possible kinetic energy, thereby minimizing collector dissipation and maximizing overall efficiency

3.  To prevent backstreaming of both reflected primary electrons and secondary electrons.

The design of the collector required optimization of the shape, position, and depression potential of each electrode. This optimization was performed during the previous study program.[1] Figure 15 is a reproduction of a computer-generated plot of the collector design for the 673H. The solid lines are trajectories and the dashed lines are equipotentials. The spent beam, which enters from the left, is made up of six energy groups with four rays each. The depression increases with distance into the collector. The depression voltages were chosen to be 50, 81, 88 and 97 percent of the cathode voltage from the energy distribution calculations of the spent beam.
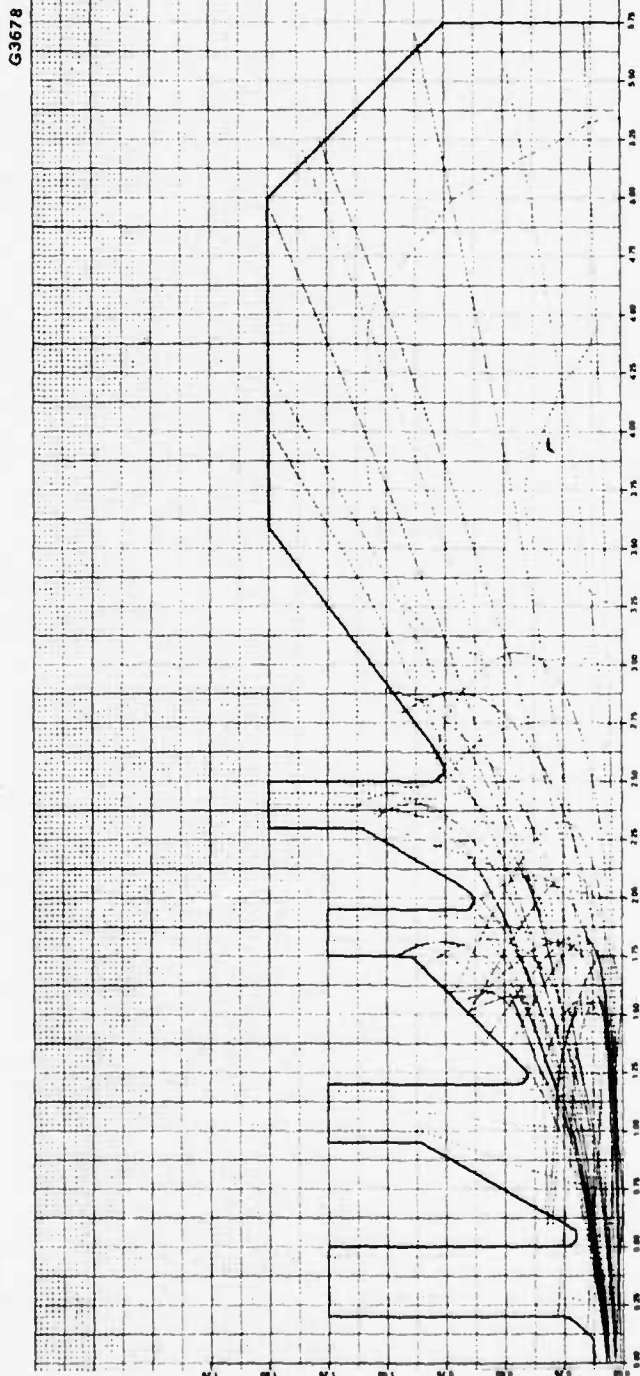
Figure 15   Four-stage depressed collector for the multitone tube (scale in inches).

28

Because of the large power dissipation and the fairly high electrode voltages required by the electrical design, the thermal and mechanical design of the collector was the most complex and critical portion of the 673H fabrication program.

The primary design criteria for this collector are to provide the electrical standoff for the four electrodes and at the same time provide a good thermal path out to the air-cooled fins. To achieve these requirements, the electrodes are completely enclosed within a ceramic cylinder. This ceramic will provide both electrical isolation and thermal conduction in the radial direction for the collector elements. With this technique, the electrical standoff for the collector is located within the vacuum envelope, eliminating the possibility of external contamination of the insulator surface. The electrical connections are made through conventional high voltage feedthroughs.

A preliminary layout of the initial concept of the collector design is shown in Figure 16. The individual electrodes are brazed to metallized bands on the inside of the ceramic cylinder. The electrodes are thin to relieve the stresses caused by the differential thermal expansions between the copper electrodes and the beryllia ceramic. The feedthroughs are located in a separate weld ring located at the front of the collector near the output pole piece. This arrangement results in the shortest lengths of the connecting leads. The cooling fins are brazed to the outside of the metallized ceramic cylinder.

Drawings of detail parts were begun for this initial collector configuration. However, when the thermal calculations were made for the maximum expected incident beam power, it was found that the temperature rise from the ceramic wall to the snout of the electrode would be about 1300°C, even though copper is an excellent conductor. This was entirely

G4500
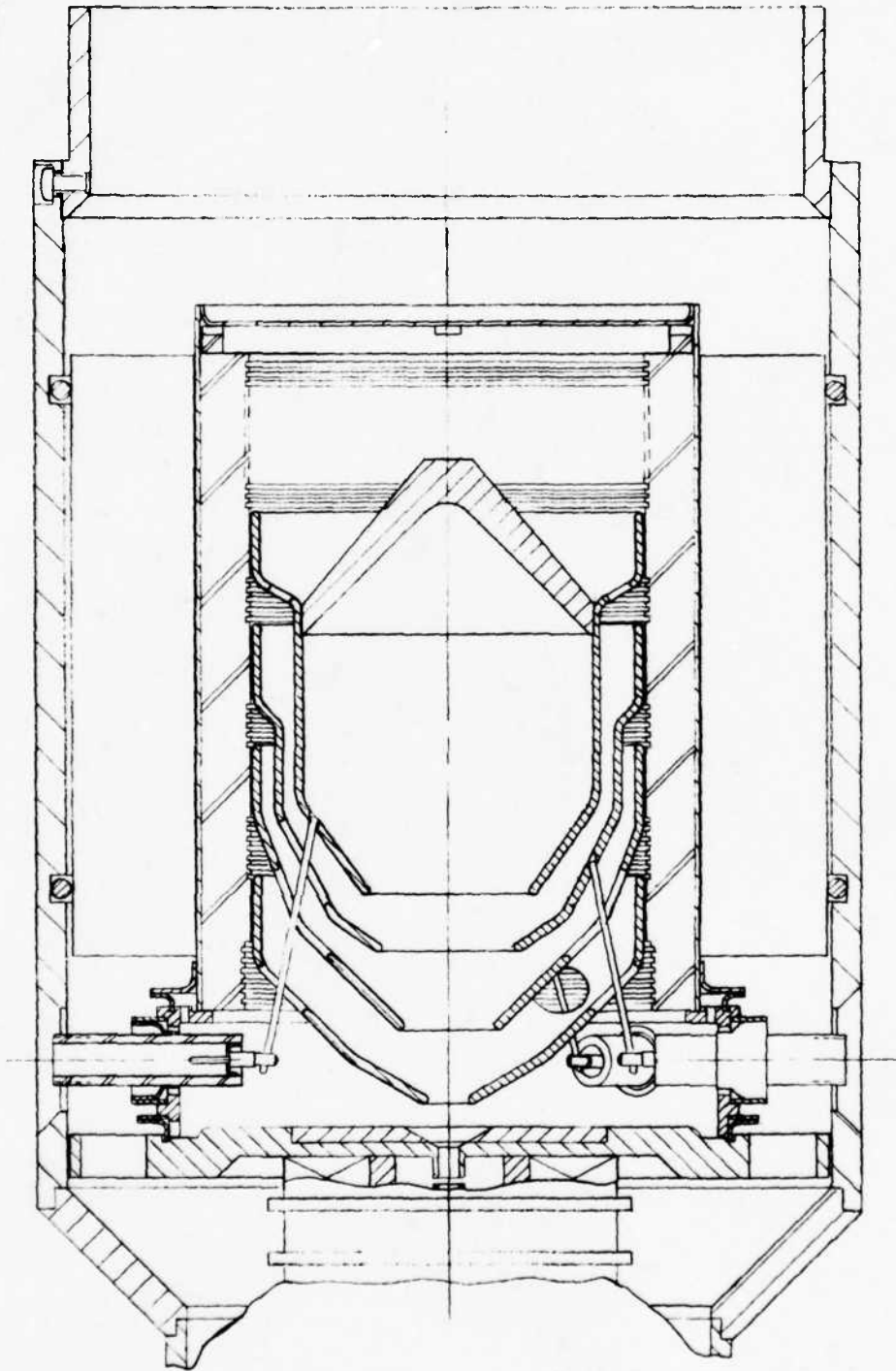


Figure 16  Layout of preliminary four-stage depressed collector for the 673H.

30

too high. Therefore, the layout of the collector was modified to make the electrodes as thick as possible in the axial direction and as short as possible in the radial direction, while maintaining the shapes of the snouts of the electrodes required for good electrical performance. This configuration necessitated running the feedthroughs out at the back end of the collector. A layout of this arrangement is shown in Figure 17. Because the spacing for the leads is tighter with the feedthroughs at the back, the leads are enclosed in ceramic tubing for extra insulation. The shape of the large ceramic cylinder was modified to accommodate this new configuration.

This final design evolved after a series of electrode and ceramic shapes was investigated. Thermal calculations were made for the various interim configurations. The results for the final design are summarized in Table 5. Since the incident beam powers on the various electrodes change depending upon the particular tube operating parameters, three different cases are tabulated. These cases represent the highest electrode power that is expected under any operating condition (plus an extra safety factor of approximately 20 percent). Case I corresponds to operation of the low end of the frequency band, Case II corresponds to the center of the band and Case III corresponds to the high frequency end. In all three cases, the RF drive level is that which gives a carrier-to-IM ratio of 20 dB. (The beam current intercepted on the fourth electrode is actually higher when the tube is operated without RF drive applied. However, the power is not as high as for Case III, because with RF some of the electrons are accelerated and have greater energy than they would have without RF drive.) As shown in Table 5, the highest calculated electrode temperature is 407ºC on electrode number 2. This is a conservative design value. For the calculations, an inlet air temperature of 38ºC with an air flow of 250 CFM was assumed. This air flow can be supplied with a fan power of 0.17 BHP.
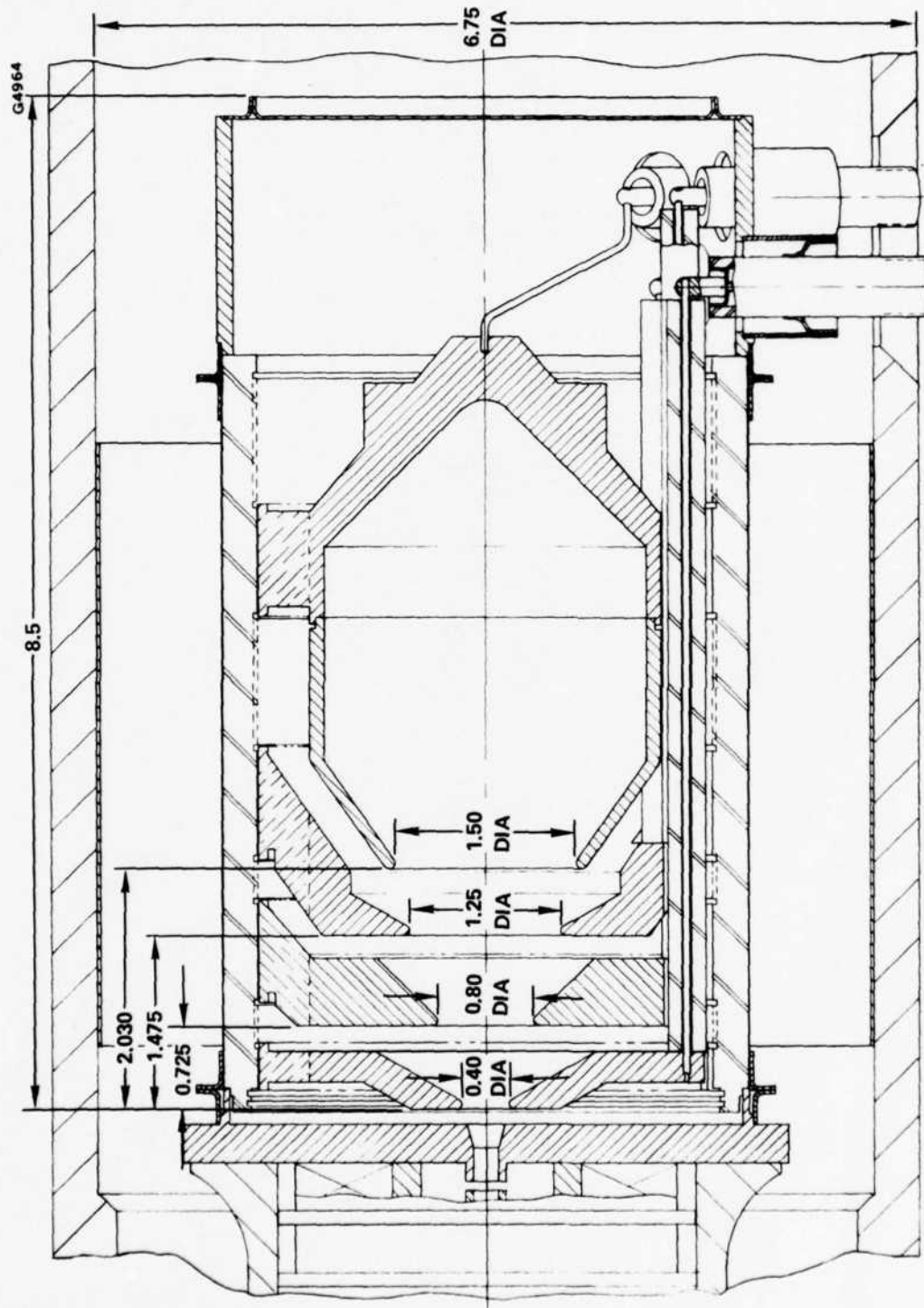
Figure 17   Schematic layout of four-stage depressed collector for 673H. Dimensions are in inches.

32

## TABLE 5

### MAXIMUM COLLECTOR ELECTRODE TEMPERATURES
### FOR WORST CASE OPERATING CONDITIONS

| | | Beam Power Per Electrode (Watts) | Maximum Temperature of Electrode ($^{o}C$) | Operating Condition |
|---|---|---|---|---|
| Case I | Electrode #1 | <u>500</u> | <u>257</u> | |
| | Electrode #2 | 200 | 174 | Low Frequency End |
| | Electrode #3 | <u>2000</u> | <u>402</u> | |
| | Electrode #4 | 1000 | 305 | |
| Case II | Electrode #1 | 400 | 236 | |
| | Electrode #2 | <u>2200</u> | <u>407</u> | Inter-mediate Frequency |
| | Electrode #3 | 500 | 266 | |
| | Electrode #4 | 1200 | 347 | |
| Case III | Electrode #1 | 300 | 214 | |
| | Electrode #2 | 1800 | 369 | High Frequency End |
| | Electrode #3 | 700 | 285 | |
| | Electrode #4 | <u>1500</u> | <u>379</u> | |

An unanswered question that remained was whether or not the collector-electrode assembly could be successfully brazed without cracking the ceramic insulator or leaving gaps at the braze interface. In order to relieve the stresses due to the differential thermal expansions of the ceramic insulator and the copper electrodes, a series of offset radial slots is cut into the outer diameter of the electrodes. This allows some flexibility in the electrodes without drastically reducing the thermal conductivity in the radial direction.

In order to establish the feasibility of the design, a dummy collector assembly was brazed. This assembly consisted of a short length of ceramic tubing, metallized on the inner diameter, and one disc with machined slots to simulate the collector electrode. The disc was annealed copper, as it would be in the actual electrode. The first braze attempt was unsuccessful; many of the electrode fingers did not braze to the ceramic wall. It was felt that this was because the soft, annealed copper fingers were bent away from the wall, as the assembly was heated, by the braze material that was inserted between the fingers and the ceramic.

A second dummy electrode assembly was brazed, for which a thinner braze shim was used and greater care was taken in the placement of the braze material. The braze turned out satisfactorily. Figure 18 is a photograph of the brazed, simulated collector assembly. All of the fingers are brazed to the metallized ceramic with continuous braze fillets. The assembly has been temperature cycled several times, both to the bakeout temperature (500 to 525°C) and to the maximum expected operating temperature (200 to 300°C). There has been no evidence of cracking or pulling away of the copper fingers from the ceramic.

Figure 19 shows the beryllia collector insulator. The insulator is metallized completely on the outside so that the cooling fins and seal

34
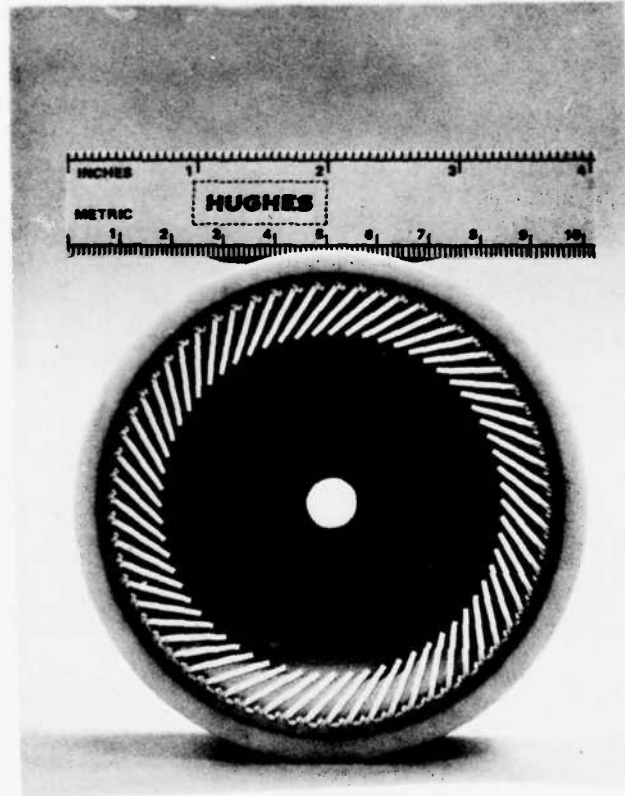
Figure 18   673H simulated collector electrode to
ceramic brazed assembly.

Figure 19    Metalized beryllia insulator for 673H
            collector.

rings can be brazed directly to the ceramic. The inside of the insulator has alternating clear and metallized ceramic strips to braze the individual collector electrodes and provide electrical isolation between them.

The collector electrode, which are machined from solid copper, are shown in Figure 20. The stress relief slots can be seen on the periphery of each electrode. Figure 21 shows a closer view of the third electrode from the back side. The design of the relief slots can be seen in greater detail.

The major portion of the collector is assembled at one time using an elaborate braze fixture, where electrodes and leads are attached to the inside of the ceramic and the cooling fins and weld rings are attached to the outside. A second weld ring assembly accommodates the feedthrough insulators for connecting to each collector electrode. Figure 22 is an end view of the completed collector with the feedthrough assembly welded on to the main collector body. The feedthroughs are attached to the electrodes using ceramic tubing for insulation.

E3156
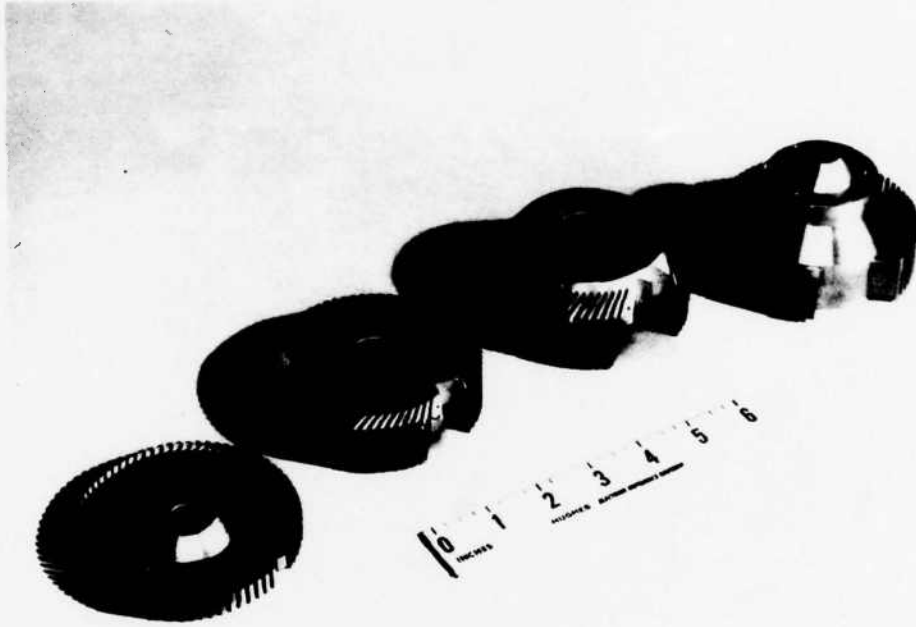
Figure 20  673H Copper collector electrodes.
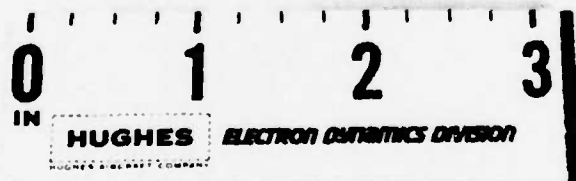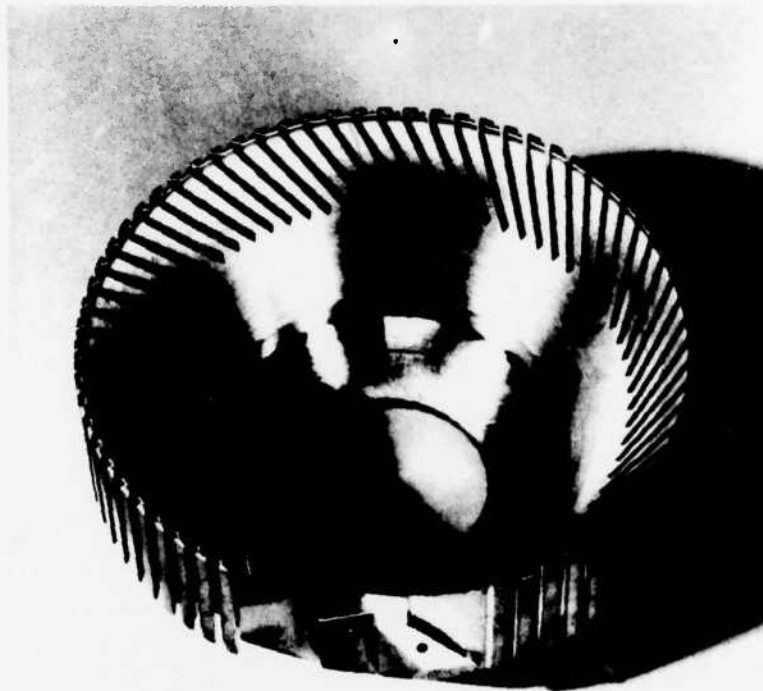
Figure 21    Closeup of third collector electrode.
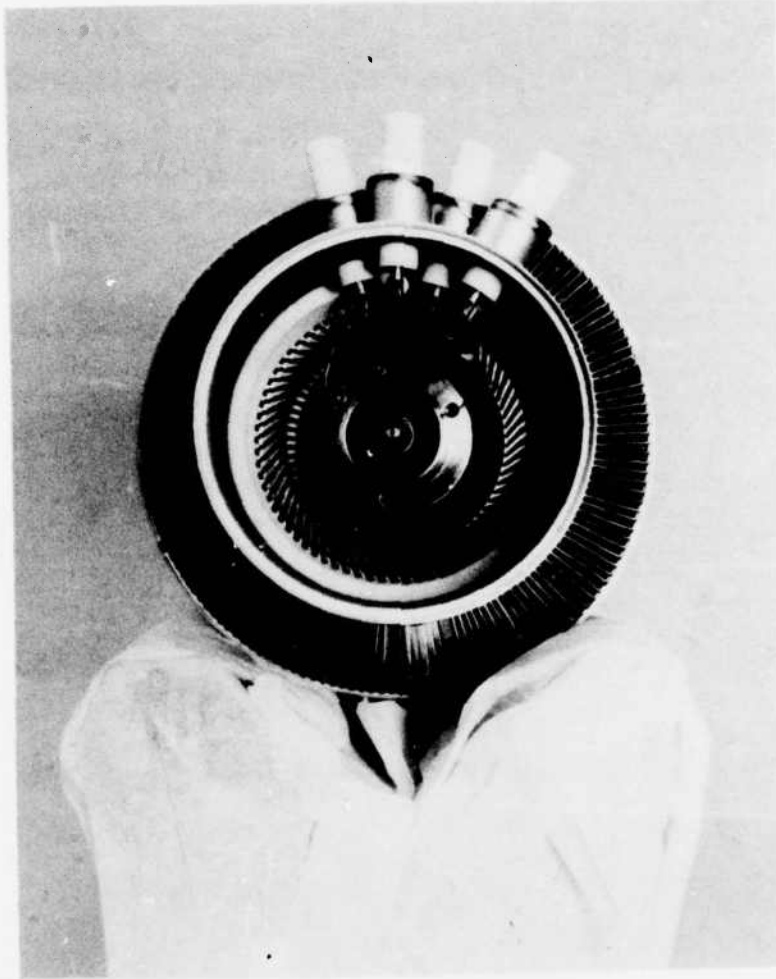
Figure 22    End view of completed 4-stage
collector assembly.

## 5.0 TUBE PERFORMANCE

The experimental 673H tube was assembled, processed, and tested at low
duty cycle.  The completed tube before processing is shown in Figure 21
resting on V blocks.  The RF interaction circuit is conventional coupled-
cavity brazed construction with copper cavity spacers and iron circuit
webs, which serve as pole pieces for the periodic permanent magnet focus-
ing.  The circuit incorporates a coaxial RF input window and a poker chip
waveguide output window.  These are welded to the circuit after the
circuit braze has been completed.  A set of fins is brazed directly to
the output pole piece to effectively cool that area in the presence of
the high beam current interception that is predicted during maximum
dpressed collector voltage conditions.

The isolated anode electron gun is shown at the right of the picture.
It is welded to the circuit assembly by heliarc welds at Kovar weld
flanges.  The area of the RF circuit between the electron gun and the
coaxial input coupler is the beam scraper section, which consists of
four solid copper drift cavities that can accommodate any excess beam
interception that might occur in that area.

The tube incorporates a 0.2-liter/sec appendage ion pump, which is
attached to the pump out tubing at the output waveguide coupler.

The four-stage, air cooled, depressed collector is at the left of Fig-
ure 23.  It is attached to the circuit by heliarc welds.  The four
individual high voltage feedthroughs are at the extreme left, beyond
the cooling fins on the collector body.

Figure 24 is a closeup of the collector end of the tube showing the
feedthroughs and cooling fins in greater detail.  The end of the collec-
tor is sealed by welding on a flanged cover as shown.

41
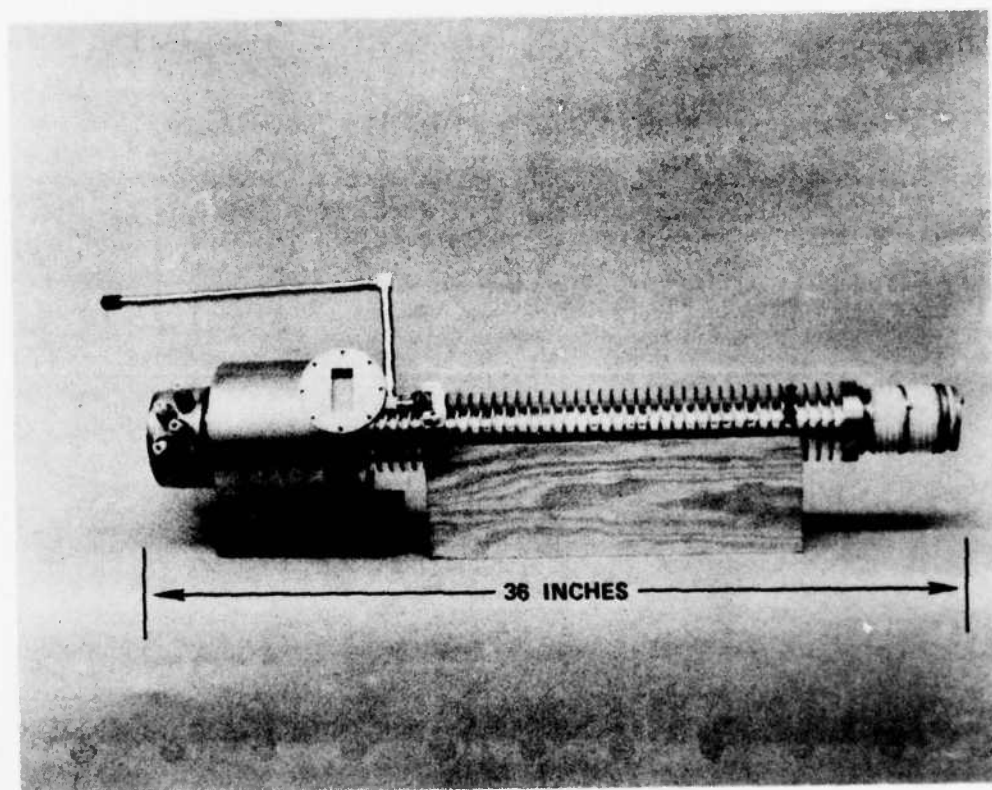
Figure 23   Completed 673H tube ready for processing.

E3160
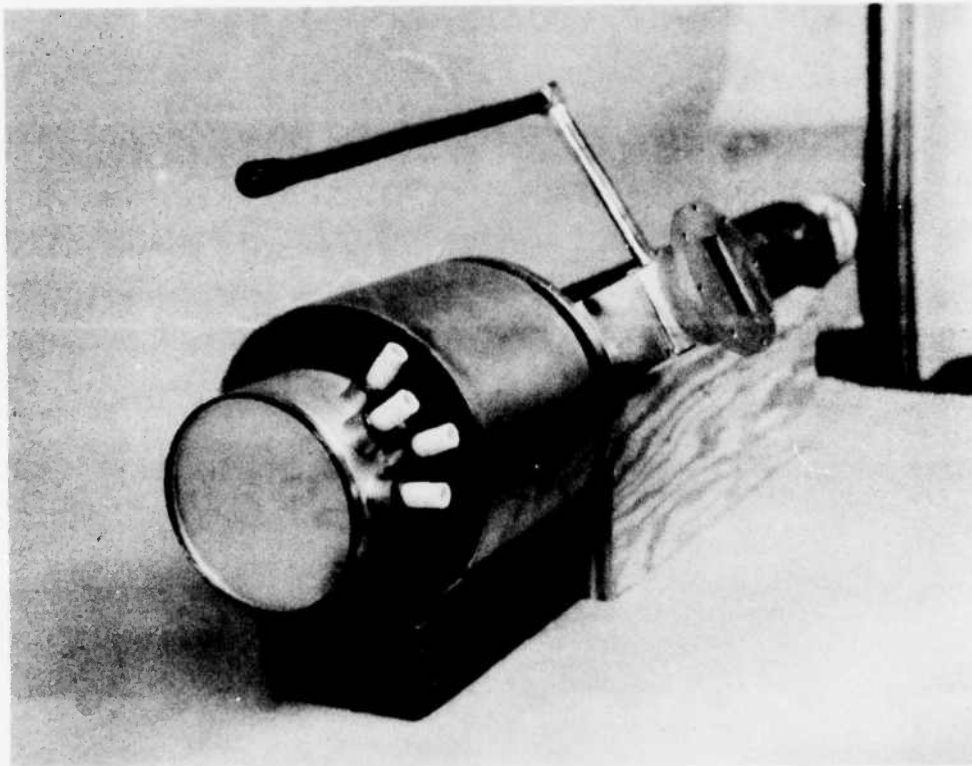


Figure 24  End view of 673H showing details of collector
cooling fins and high voltage feedthroughs.

After processing was completed, the exhaust tubing was pinched off; there were no vacuum leak problems. The tube was then placed on the test stand. The collector insulators stood off the required operating voltages.

The focusing magnets were installed and shunts were applied to optimize the beam transmission. The tube was operated on a cathode pulsed modulator with the anode connected to the body electrically. It was run at 0.002 duty cycle. The body cooling fins and final packaging of the tube were not installed. (They cannot be put on until the magnetic field shunting has been completed, because the magnets are inaccessible after the body fins are in place. The tube cannot be operated at high duty cycle without the proper air cooling applied.) The tube was operated with all of the collector electrodes at ground (body) potential. The heaters were run at 10.5 V and 2.5 A. The cathode voltage was set at -24 kV. Under these conditions, the cathode current was 1.2 A. This is a beam perveance of 0.32 microperv, which corresponds closely to the lower voltage data taken earlier on the gun in the demountable beam tester.

The beam transmission was 98 percent without RF input (0.024 A body current). Power output versus frequency with constant values of input drive is shown in Figure 25. The transmission at 30-dBM input near saturation was 90 percent. (However, this would not be a normal operating point for a multitone tube operating at small signal to obtain good intermodulation products.) This performance agreed fairly well with the basic parameters of the theoretical design.

A complete set of data was not compiled for this tube because the testing facilities were not available and funding was insufficient.

44
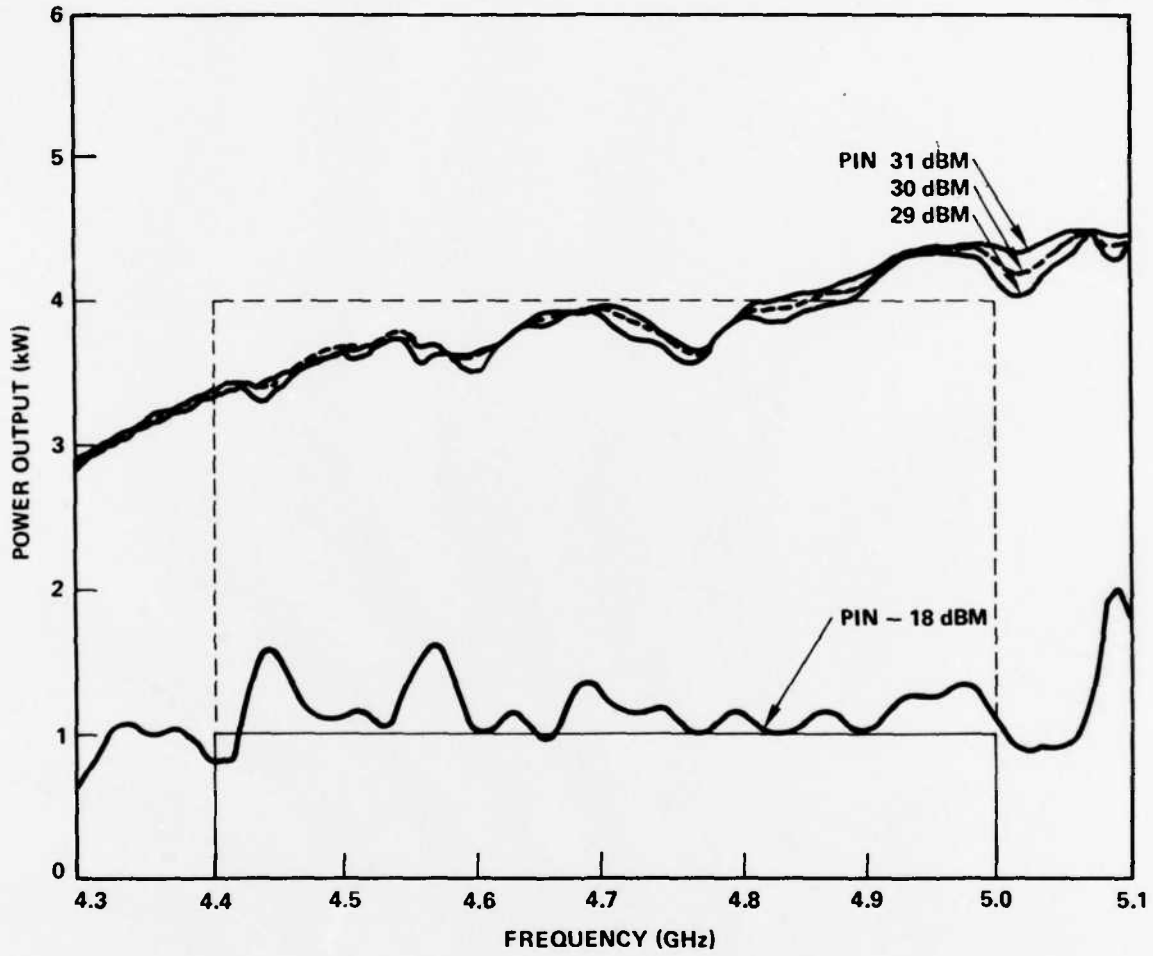
Figure 25    Power output versus frequency of 673H at −24 kV
             cathode voltage.

45

## 6.0 CONCLUSIONS AND RECOMMENDATIONS

In the course of this development program the mechanical design of a sophisticated, high power, air cooled, coupled-cavity, permanent magnet focused traveling-wave tube, incorporating a complicated four-stage depressed collector, was accomplished. An experimental model of the 673H tube was successfully constructed, and a limited amount of performance data was obtained.

This tube had been specifically designed for operation in the troposcatter communications frequency band to obtain optimum performance while amplifying multiple signals. To minimize products which result from nonlinear operation, the tube is to be operated in the linear region below saturation; tube efficiency is enhanced by the multiple-stage depressed collector.

This program demonstrated that this type of tube could be constructed, although the requirement that the tube air cooled resulted in a complicated and expensive collector design.

As far as the evaluation of the tube was carried out, there were no obvious problems. The tube performed as predicted. However, because the testing of the tube had to be stopped, many of the major design objectives were not investigated.

It is recommended that complete testing of the tube be funded. This would include the following:

1. Low duty performance should be investigated over a wider range of operating beam voltages and RF drive levels. Additional beam focusing improvement should be investigated by shunting the focusing magnets. Phase and gain compression versus RF input power curves should be obtained in order to

compare the actual performance characteristics of the 673H
against the values that were assumed in the original
calculations.

2.  The performance of the depressed collector should be evaluated
    by applying the required voltages to the collector electrodes
    and measuring the beam current distribution under various
    operating conditions.  This can be done at low duty cycle.
    From this data the efficiency can be calculated.

3.  The intermodulation distortion characteristics with multiple
    input signals should be measured.  To be meaningful, at least
    three simulataneous signals should be used.  It is anticipated
    that separation of the intermodulation products will be diffi-
    cult if this measurement is performed pulsed at low duty
    cycle.

4.  The thermal capability of the air cooled design should be
    evaluated by raising the duty cycle.  The body cooling fins
    and external packaging of the tube will have to be installed
    and the required cooling air applied.  If possible, CW opera-
    tion should be achieved.  Then the multitone intermodulation
    measurements could be made more accurately and compared with
    the theoretical predictions.

If the testing program is completed successfully, the tube could be
used in an actual system configuration.  More important, the multitone
design approach could be applied to other tube designs for communica-
tions and radar systems.

47

# REFERENCES

1.    I. Tammaru, "Multitone Troposcatter Tube (G-Band)," Research and
      Development Technical Report ECOM-75-1283-F, July 1975, U.S.
      Army Electronics Command.

2.    J.R. Pierce, Theory and Design of Electron Beams, D. Van Norstrand
      Co., Inc., 1954.

3.    W.B. Herrmansfeldt, Electron Trajectory Program.  SLAC-166 (A)
      UC-28, Stanford Linear Accelerator Center, Stanford University,
      Stanford, CA 94305.  Prepared for U.S. Atomic Energy Commission
      under contract AT(04-3)-515, September 1943.  Available from
      National Technical Information Service, U.S. Department of
      Commerce, 5285 Port Royal Road, Springfield, VA 22151.

4.    K. Amboss, "Verification and Use of Hermann's Optical Theory of
      Velocity Effects in Electron Beams in the Low Perveance Regime,"
      IEEE Transactions of The Electron Devices Group, Volume ED-II,
      No. 10, October 1964.

5.    K. Amboss, "The Analysis of Dense Electron Beams Advances in
      Electronics and Electron Physics," Vol. 26, Academic Press, Inc.,
      New York, 1969.

48

# DISTRIBUTION LIST

| | No. Copies | | No. Copies |
|---|---|---|---|
| Defense Documentation Center<br>ATTN: DDC-TCA<br>Cameron Station (Bldg. 5)<br>Alexandria, VA 22314 | 12 | Commander<br>Naval Electronics Laboratory Center<br>Attn: Library<br>San Diego, CA 92152 | 1 |
| Code R123, Tech Library<br>DCA Defense Comm Engrg Ctr<br>1860 Wiehle Ave.<br>Reston, VA 22090 | 1 | CDR, Navar Surface Weapons Center<br>White Oak Laboratory<br>Attn: Library, Code WX-21<br>Silver Spring, MD 20910 | 1 |
| Defense Communications Agency<br>Technical Library Center<br>Code 205 (P.A. Tolovi)<br>Washington, DC 20305 | 1 | Commandant, Marine Corps<br>HQ, US Marine Corps<br>Attn: Code LMC<br>Washington, DC 20380 | 2 |
| Office of Naval Research<br>Code 427<br>Arlington, VA 22217 | 1 | HQ, US Marine Corps<br>Attn: Code Ints<br>Washington, DC 20380 | 1 |
| Gidep Engineering & Support Dept.<br>TE Section<br>PO Box 398<br>Norco, CA 91760 | 1 | Command, Control & Communications Div<br>Development Center<br>Marine Corps Development & Educ Comd<br>Quantico, VA 22134 | 1 |
| Director<br>Naval Research Laboratory<br>Attn: Code 2627<br>Washington, DC 20375 | 1 | Rome Air Development Center<br>Attn: Documents Library (TILD)<br>Griffiss AFB, NY 13441 | 1 |
| HQ ESD (DRI)<br>L. G. Hanscom AFB<br>Bedford, MA 01731 | 1 | Commandant<br>US Army Military Police School<br>Attn: ATSJ-CD-M-C<br>Fort McClellan, AL 36201 | 3 |
| HQ, Air Force Systems Command<br>Attn: DLCA<br>Andrews AFB<br>Washington, DC 20331 | 1 | Commander<br>US Army Intelligence Center & School<br>Attn: ATSI-CD-MD<br>For Huachuca, AZ 85613 | 2 |
| Cdr, MIRCOM<br>Redstone Scientific Info Center<br>Attn: Chief, Document Section<br>Redstone Arsenal, AL 35809 | 1 | Commander<br>HQ Fort Huachuca<br>Attn: Technical Reference Div<br>Fort Huachuca, AZ 85613 | 1 |

| | No. Copies | | No. Copies |
|---|---|---|---|
| Commandant<br>US Army Aviation Center<br>Attn: ATZQ-D-MA<br>Fort Rucker, AL 36362 | 3 | Deputy for Science & Technology<br>Office, Assist Sec Army (R&D)<br>Washington, DC 20310 | 1 |
| Director, Ballistic Missile Def<br>Advanced Technology Center<br>Attn: ATC-R, PO Box 1500<br>Huntsville, AL 35807 | 1 | Director<br>US Army Material Systems Analysis Act.<br>Attn: DRXSY-T<br>Aberdeen Proving Ground, MD 21005 | 1 |
| HODA(DAMA-ARZ-D)<br>Dr. F.D. Verderame<br>Washington, DC 20310 | 1 | Commander<br>US Army Tank-Automotive Command<br>Attn: DRDTA-RH<br>Warren, MI 48090 | 1 |
| Commandant<br>US Army Signal School<br>Attn: ATSN-CTD-MS<br>Fort Gordon, GA 30905 | 1 | CDR, US Army Aviaion Systems Command<br>Attn: DRSAV-G<br>PO Box 209<br>St. Louis, MO 63166 | 1 |
| Director of Combat Developments<br>US Army Armor Center<br>Attn: ATZK-CD-MS<br>Fort Knox, KY 40121 | 2 | Commander, Picatinny Arsenal<br>Attn: SARPA-FR-S<br>Bldg. 350<br>Dover, NJ 07801 | 2 |
| Commandant<br>US Army Ordnance School<br>Attn: ATSL-CD-OR<br>Aberdeen Proving Ground, MD 21005 | 2 | Commander<br>Picatinny Arsenal<br>Attn: SARPA-ND-A-4 (Bldg. 95)<br>Dover, NJ 07801 | 1 |
| CDR, Harry Diamond Laboratories<br>Attn: Library<br>2800 Powder Mill Road<br>Adelphia, MD 20783 | 1 | Commander<br>Picatinny Arsenal<br>Attn: SARPA-TS-S 59<br>Dover, NJ 07801 | 1 |
| Director<br>US Army Ballistic Research Labs<br>Attn: DRXBR-LB<br>Aberdeen Proving Ground, MD 21005 | 1 | Project Manager, Rembass<br>Attn: DRCPM-RBS<br>Fort Monmouth, NJ 07703 | 2 |
| Harry Diamond Laboratories<br>Dept of Army<br>Attn: DELHD-RCB (Dr. J. Nemarich)<br>2800 Powder Mill Road<br>Adelphi, MD 20783 | 1 | Commandant<br>US Army Air Defense School<br>Attn: ATSA-CD-MC<br>Fort Bliss, TX 79916 | 1 |
| General Electric Company<br>Research & Development Division<br>Attn: Dr. T. Mihran<br>Schenectady, NY 12301 | 1 | Commander<br>US Army Nuclear Agency<br>Fort Bliss, TX 79916 | 1 |

| | No.<br>Copies | | No.<br>Copies |
|---|---|---|---|
| Commander<br>US Army Satellite Communications<br>Attn: DRCPM-SC-5 (A. Wachtenheim)<br>Fort Monmouth, NJ 07703 | 2 | Commander, HQ MASTER<br>Technical Information Center<br>Attn: Mrs. Ruth Reynolds<br>Fort Hood, TX 76544 | 1 |
| TRI-TAC Office<br>Attn: TT-SEL<br>Fort Monmouth, NJ 07703 | 1 | Commander, Darcom<br>Attn: DRCDE<br>5001 Eisenhower Ave.<br>Alexandria, VA 22333 | 1 |
| CDR, US Army Research Office<br>Attn: DRXRO-IP<br>PO Box 12211<br>Research Triangel Park, NC 07709 | 1 | CDR, US Army Signals Warfare Lab<br>Attn: DELSW-OS<br>Arlington Hall Station<br>Arlington, VA 22212 | 1 |
| Commandant<br>US Army Inst for Military Assistance<br>Attn: ATSU-CTD-MO<br>Fort Bragg, NC 28307 | 1 | Commander<br>US Army Engineer Topographic Labs<br>Attn: ETL-TD-EA<br>Fort Belvoir, VA 22060 | 1 |
| CDR, US Army Tropic Test Center<br>Attn: STETC-MO-A (Tech Library)<br>Drawer 942<br>Fort Clayton, Canal Zone 09827 | 1 | National Bureau of Standards<br>Bldg. 225, RM A-331<br>Attn: Mr. Leddy<br>Washington, DC 20231 | 1 |
| Division Chief<br>Meterology Division<br>Counterfire Department<br>Fort Sill, OK 73503 | 2 | Advisory Group on Electron Devices<br>201 Varick Street, 9th Floor<br>New York, New York 10014 | 2 |
| TACTEC<br>Ballelle Memorial Institute<br>505 King Avenue<br>Columbus, OH 43201 | 1 | Plastics Tech Eval Center<br>Picatinny Arsenal, Bldg. 176<br>Attn: Mr. A. M. Anzalone<br>Dover, NJ 07801 | 1 |
| Ketron, Inc.<br>Attn: Mr. Frederick Leuppert<br>1400 Wilson Blvd., Architech Bldg.<br>Arlington, VA 22209 | 2 | Metals and Ceramics Info Center<br>Battelle<br>505 King Avenue<br>Columbus, OH 43201 | 1 |
| Commander<br>US Army Logistics Center<br>Attn: ATCL-MC | 2 | Commander<br>US Army Communications R&D Command<br>Fort Monmouth, NJ 07703 | 1 |
| Comsat Laboratories<br>Attn: R. Strauss<br>Clarisburg, Maryland 20734 | 1 | 1 DRDCO-COM-RO<br>1 USMC-LNO<br>1 ATFE-LO-EC | |

|  | No. Copies |  | No. Copies |
|---|---|---|---|
| Director, Night Vision Laboratory<br>US Army Electronics R&D Command<br>Attn: DELNV-D<br>Fort Belvoir, VA 22060 | 1 | Commander<br>US Army Communications & Electronic<br>Material Readiness Command | 1 |
| | | DRSEL-PL-ST | 1 |
| CDR/DIR, Atmospheric Sciences Lab<br>US Army Electronics R&D Command<br>Attn: DELAS-SY-S<br>White Sands Missile Range, NM 88002 | 1 | DRSEL-MA-MP<br>**DRSEL-MS-TI<br>DRSEL-PP-I-PI<br>DRSEL-PA<br>DRSEL-LW-LS | 1<br>2<br>1<br>2<br>1 |
| Chief<br>OFC of Missile Electronic Warfare<br>Electronic Warfare Lab, ERADCOM<br>Fort Meade, MD 20755 | 1 | Cindas<br>Purdue Industrial Research Park<br>2595 Yeager Road<br>W. Lafayette, IN 47096 | 1 |
| Commander<br>US Army Electronics R&D Command<br>Fort Monmouth, NJ 07703 | | MIT - Lincoln Laboratory<br>Attn: Library (RM A-082)<br>PO Box 73 | 1 |
| DELEW-D<br>DELCS-D | 1<br>3 | Lexington, MA 02173 | |
| DELAS-D | 1 | NASA Scientific & Tech Info Facility | 1 |
| DELSD-AS | 1 | Baltimore/Washington Intl Airport | |
| DELET-DD | 1 | PO Box 8757, MD 21240 | |
| *DELET-BM (GWurthmann) | 3 | | |
| DELET-P | 1 | ITT Electron Tube Division | 1 |
| DELSD-L (Tech Lib) | 1 | Box 100 | |
| DELSD-D | 1 | Attn: Mr. R. Wertman | |
| DELET-D | 1 | Easton, PA 18042 | |
| Originating Office | 25 | | |
| | | Litton Industries | 1 |
| Raytheon Company<br>Microwave & Power Tube Division<br>Foundry Avenue<br>Attn: Mr. D. Winsor<br>Waltham, MA 02154 | 1 | Electron Tube Division<br>960 Industrial Road<br>Attn: Mr. R. Phillips<br>San Carlos, CA 94070 | |
| | | Varian Associates | 1 |
| Watkins-Johnson<br>Electron Device Division<br>3333 Hillview Avenue<br>Attn: Dr. K. Niclos<br>Palo Alto, CA 94304 | 1 | Mircrowave Tube Division<br>611 Hansen Way<br>Attn: Dr. E. Lien<br>Palo Alto, CA 94303 | |
| | | Hughes Aircraft Co. | 1 |
| Warnecke Electron Tubes, Inc.<br>175 W. Oakton Street<br>Attn: Dr. O. Doehler<br>Des Plains, IL 60018 | 1 | Electron Dynamics Division<br>3100 W. Lomita Blvd.<br>Attn: Dr. J. Mendel<br>Torrance, CA 90509 | |

Redstone Arsenal, AL 35809          Fort Huachuca, AZ 85613

Adelphi, MD 20783

General Electric Company                     1    Commander                              1
Research & Development Division                    US Army Nuclear Agency
Attn:  Dr. T. Mihran                               Fort Bliss, TX 79916
Schenectady, NY 12301

Attn:  R. Strauss
Clarisburg, Maryland 20734                    1  ATFE-LO-EC